Inorganic Chemistry

Article

pubs.acs.org/IC

Interaction of Antidiabetic Vanadium Compounds with Hemoglobin and Red Blood Cells and Their Distribution between Plasma and Erythrocytes

Daniele Sanna,[†] Maria Serra,[†] Giovanni Micera,[‡] and Eugenio Garribba*[,‡]

[†]Istituto CNR di Chimica Biomolecolare, Trav. La Crucca 3, I-07040 Sassari, Italy

[‡]Dipartimento di Chimica e Farmacia, and Centro Interdisciplinare per lo Sviluppo della Ricerca Biotecnologica e per lo Studio della Biodiversità della Sardegna, Università di Sassari, Via Vienna 2, I-07100 Sassari, Italy

Supporting Information

ABSTRACT: The interaction of $V^{IV}O^{2+}$ ion with hemoglobin (Hb) was studied with the combined application of spectroscopic (EPR), spectrophotometric (UV−vis), and computational (DFT methods) techniques. Binding of Hb to $V^{IV}O^{2+}$ in vitro was proved, and three unspecific sites (named α, β, and γ) were characterized, with the probable coordination of His−N, Asp−O^-, and Glu−O^- donors. The value of log β for (VO)Hb is 10.4, significantly lower than for human serum apo-transferrin (hTf). In the systems with $V^{IV}O$ potential antidiabetic compounds, mixed species *cis*-VOL_2(Hb) (L = maltolate (ma), 1,2-dimethyl-3-hydroxy-4(1*H*)-pyridinonate (dhp)) are observed with equatorial binding of an accessible His residue, whereas no ternary complexes are observed with acetylacetonate (acac). The experiments of uptake of $[VO(ma)_2]$, $[VO(dhp)_2]$, and $[VO(acac)_2]$ by red blood cells indicate that the neutral compounds penetrate the erythrocyte membrane through passive diffusion, and percent amounts higher than 50% are found in the intracellular medium. The biotransformation of $[VO(ma)_2]$, $[VO(dhp)_2]$, and $[VO(acac)_2]$ inside the red blood cells was proved. $[VO(dhp)_2]$ transforms quantitatively in *cis*-$VO(dhp)_2$(Hb), $[VO(ma)_2]$ in *cis*-$VO(ma)_2$(Hb), and *cis*-$VO(ma)_2$(Cys-S^-), with the equatorial coordination of a thiolate-S^- of GSH or of a membrane protein, and $[VO(acac)_2]$ in the binary species $(VO)_x$Hb and two $V^{IV}O$ complexes with formulation $VO(L^1,L^2)$ and $VO(L^3,L^4)$, where L^1, L^2, L^3, and L^4 are red blood cell bioligands. The results indicate that, in the studies on the transport of a potential pharmacologically active V species, the interaction with red blood cells and Hb cannot be neglected, that a distribution between the erythrocytes and plasma is achieved, and that these processes can significantly influence the effectiveness of a V drug.

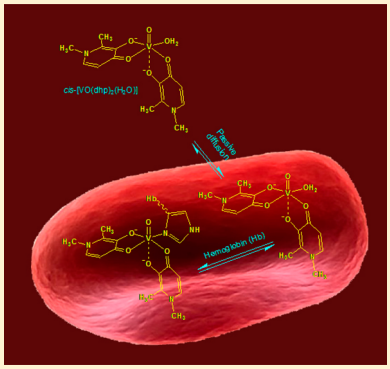

INTRODUCTION

Vanadium plays a number of roles in the biological systems and has been found in many naturally occurring compounds.[1] In humans, V compounds exhibit a wide variety of pharmacological properties, and many complexes have been tested as antiparasitic, spermicidal, antiviral, anti-HIV, antituberculosis, and antitumor agents.[2] Particularly, vanadium has been proved to be one of the most efficient metal ions with potential antidiabetic activity.[3] Because of this insulin-like effect, the most important pharmacological application of vanadium compounds is their potential use in the therapy of patients suffering from type II diabetes mellitus.[4] A class of very promising complexes consists of neutral $V^{IV}O$ complexes with bidentate anionic ligands L^- (L is named also organic *carrier*) with composition VOL_2. Bis(maltolato)oxidovanadium(IV) (or BMOV) became the benchmark compound for the new molecules with antidiabetic action,[4,5] and its derivative bis(ethylmaltolato)oxidovanadium(IV) (or BEOV) got to phase IIa of the clinical trials.[6]

The biotransformation of the antidiabetic complexes in the blood, the mechanism with which vanadium is transported to the target organs, and the in vivo form are not fully known and have been recently reviewed.[3,7−10] The transformation of a V compound in the organism and the distribution between the bioligands of the blood is an important aspect of the drug metabolism and mechanism of action. These processes are related to the thermodynamic stability of the vanadium complexes and to the interaction with the proteins (human serum apo-transferrin (hTf), human serum albumin (HSA), and immunoglobulins (Ig)) and low molecular mass ligands (lactic acid (Hlact) and citric acid (H_3citr)) of the blood serum.[11] Until a few years ago, it was believed that all $V^{IV}O^{2+}$ ion was transported toward the target organs as binary complexes with hTf ((VO)hTf and $(VO)_2$hTf),[7−10,12] but the participation of other proteins such as HSA and immunoglobulin G (IgG) and the formation of mixed complexes between the insulin-enhancing VOL_2 compounds and hTf, HSA, or IgG has been recently demonstrated.[9,12−14] When the arrangement of V compound in aqueous solution at pH 7.4 is *cis*-octahedral,

Received: September 18, 2013
Published: January 17, 2014

   dx.doi.org/10.1021/ic402366x | *Inorg. Chem.* 2014, 53, 1449−1464

Scheme 1. Structures of the Three Potential Antidiabetic V Compounds at Physiological pH: (a) *cis*-[VO(ma)$_2$(H$_2$O)], (b) [VO(dhp)$_2$] and *cis*-[VO(dhp)$_2$(H$_2$O)] in Equilibrium with Each Other, and (c) [VO(acac)$_2$]

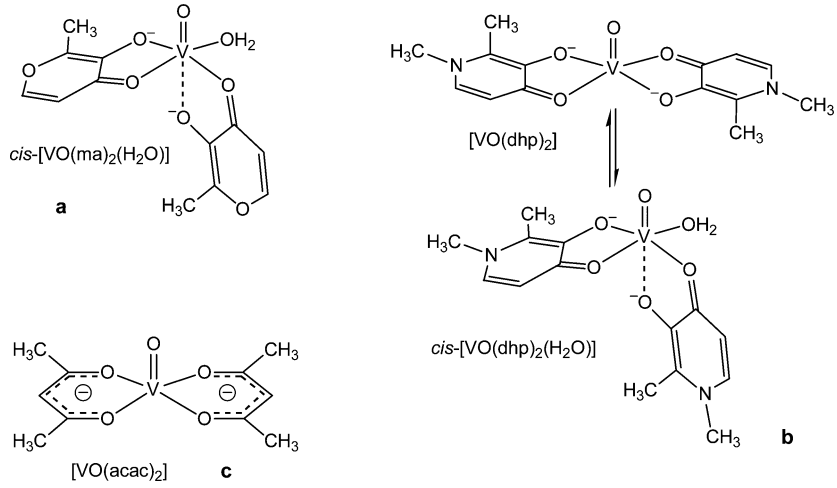

HSA and IgG form species with stoichiometry *cis*-VOL$_2$(HSA) and *cis*-VOL$_2$(IgG) through the coordination of an accessible His-N, which replaces the water molecule occupying the fourth equatorial position.[14] Concerning the type of complexes formed with hTf, no general consensus exists in the literature, and the formulation *cis*-VOL$_2$(hTf) with the coordination of a His-N in the fourth equatorial position,[14] and (VO)(hTf)(L) or (VO)$_2$(hTf)(L)$_2$, with the binding of VOL$^+$ unit at the iron binding sites, was proposed.[9,12,13d,e]

The participation of erythrocytes in the transport of inorganic $V^{IV}O^{2+}$ ion and antidiabetic VOL$_2$ compounds has been considered previously but never described in detail. It has been demonstrated that $V^{IV}O^{2+}$ ion may be transported through the erythrocyte membrane by the divalent metal transporter 1 protein (DMT1, also known as Nramp2, which carries iron into the cells of the gastrointestinal system and out of endosomes in the transferrin cycle).[15] Furthermore, Yang et al. proved that [VO(ma)$_2$] and [VO(acac)$_2$] enter the cells through passive diffusion and have an absorption kinetically quicker than $NaV^{V}O_3$,[16] which in its turn is transported through the anion channels. The amount of vanadium associated to the red blood cells is not clear,[17] and several studies were published about the distribution of V between blood serum and erythrocytes. Even if none of them appear to be definitive, the ratio depends on the rates of influx and efflux across the cell membrane, on the redox reactions in the erythrocytes between V^{V} and V^{IV} (reduction of V^{IV} to V^{III} is usually neglected), and on the binding of V^{IV} and V^{V} to the available bioligands.[18] Electrophoresis suggested that about 77% of vanadium is associated with the serum fraction, regardless of the chemical form initially injected,[18] but a general analysis of the data available in the literature suggested that in mammals the ratio between V in the plasma and erythrocytes is in the range 90:10−95:5;[19] however, experiments with $Na_3{}^{48}VO_4$ showed that the V concentration in the red blood cells can exceed that in the extracellular medium from 4- to 18-fold.[20] Furthermore, the availability to the target cells of the V associated to the erythrocytes is not known.[17]

Most of the experimental studies indicate that, inside the erythrocytes, $V^{IV}O^{2+}$ ion is bound mainly to hemoglobin (Hb),[21,22] whose concentration is about 330 mg/mL, corresponding to 5.1 mM.[23] Therefore, Hb appears to be the main candidate for the interaction with V compounds in the red blood cells. The level of $V^{IV}O^{2+}$ bound to Hb was diminished by addition of adenosine 5′-triphosphate (ATP) and 2,3-diphosphoglycerate, suggesting that other intracellular bioligands can compete with hemoglobin.[22]

In this work, the interaction of $V^{IV}O^{2+}$ ion and three important potential antidiabetic $V^{IV}O$ compounds ([VO(ma)$_2$], [VO(dhp)$_2$], and [VO(acac)$_2$], with Hma that indicates maltol, Hdhp, 1,2-dimethyl-3-hydroxy-4(1*H*)-pyridinone, and Hacac, acetylacetone, see Scheme 1) with hemoglobin and red blood cells was studied by spectroscopic (EPR spectroscopy), spectrophotometric (UV−vis), and computational (DFT methods) techniques.

The main goals of the present study were (i) the examination of the binary system $V^{IV}O^{2+}$/Hb to establish the type of interaction between $V^{IV}O^{2+}$ ion and hemoglobin; (ii) the examination of the ternary system $V^{IV}O^{2+}$/Hb/hTf to evaluate the relative strength of these two proteins toward $V^{IV}O^{2+}$; (iii) the examination of the ternary systems $V^{IV}O^{2+}$/Hb/*carrier*, where *carrier* is ma, dhp, and acac; and (iv) the examination of the uptake of [VO(ma)$_2$], [VO(dhp)$_2$], and [VO(acac)$_2$] by red blood cells to establish if and in which amount the antidiabetic V species can cross the erythrocyte membrane and which is the distribution of $V^{IV}O$ complexes between the plasma and intracellular medium. The experiments on the uptake of antidiabetic VOL$_2$ compound by red blood cells were compared to those with vanadate(V). The results may provide new insights on the transport of the potential antidiabetic V complexes in the organism and explain, at least partly, their mechanism of action and the different effectiveness. In fact, such an effectiveness depends on the amount reaching the target organs, which in its turn is related to the distribution between the blood serum and erythrocytes.

EXPERIMENTAL AND COMPUTATIONAL SECTION

Chemicals. Water was deionized prior to use through the purification system Millipore Milli-Q Academic. $V^{IV}O^{2+}$ solutions were prepared from $VOSO_4{\cdot}3H_2O$ following literature methods.[24] $NaVO_3$ was used as a source for vanadium(V). Human serum apotransferrin (hTf) and hemoglobin (Hb) were purchased from Sigma. Hb (Sigma H7379) and hTf (Sigma T4283) have a molecular mass of 64.5 and 76−81 kDa, respectively. The product specification sheet accompanying Hb states that this contains 0.31% of iron, which corresponds to a saturation of the iron sites of about 95%. Other chemicals, that is, 3-hydroxy-2-methyl-4*H*-pyran-4-one or maltol

dx.doi.org/10.1021/ic402366x | *Inorg. Chem.* 2014, 53, 1449−1464

(Hma), 1,2-dimethyl-3-hydroxy-4(1*H*)-pyridinone (Hdhp), acetylacetone (Hacac), 4-(2-hydroxyethyl)piperazine-1-ethanesulfonic acid (HEPES), 1-methyimidazole (1-MeIm), glutathione reduced (GSH), 3-mercaptopropionyl sulfonic acid (3-mps), 4-(2-pyridylazo)-resorcinol (PAR), (EDTA), $NaHCO_3$, NaCl, NaH_2PO_4, and glucose, were Aldrich or Fluka products of the highest grade available and used as received.

Preparation of the Solutions for EPR Measurements. The solutions were prepared by dissolving in ultrapure water $VOSO_4 \cdot 3H_2O$ to obtain a $V^{IV}O^{2+}$ concentration between 3.1×10^{-4} and 1×10^{-3} M. Argon was bubbled through the solutions to ensure the absence of oxygen and avoid the oxidation of $V^{IV}O^{2+}$ ion. To the solution containing the metal ion an appropriate amount of the eventual ligand (Hma, Hdhp, or Hacac) and HEPES were added. The ratio between the organic *carriers* and $V^{IV}O^{2+}$ ion was 2.

Subsequently, pH was raised to ca. 5.5, and, in the system with apotransferrin, $NaHCO_3$ was dissolved (the presence of $NaHCO_3$ as synergistic anion is necessary for vanadium coordination to hTf;[25] it is present in high excess in comparison with vanadium, and it is enough for the $V^{IV}O^{2+}$ binding, despite that a fraction of bicarbonate can be lost as CO_2 because of the low pH of the solution). To 1 mL of this solution, again carefully purged with argon, Hb and hTf were added to obtain a concentration in the range $(1.25–3.1) \times 10^{-4}$ and 2.5×10^{-4} M, respectively. Subsequently, pH was adjusted to ca. 7.4. The stabilization of the pH value indicated that the equilibrium was reached (this happens almost immediately after the addition of hTf). The final concentration of HEPES and $NaHCO_3$ was 1.0×10^{-1} and 2.5×10^{-2} M (corresponding to the concentration in the blood). EPR studies performed on the model systems prove that HEPES and $NaHCO_3$ do not interact with $V^{IV}O^{2+}$ ion at the conditions used for the experiments.

The model systems $V^{IV}O^{2+}$/*carrier*, $V^{IV}O^{2+}$/*carrier*/1-MeIm, and $V^{IV}O^{2+}$/*carrier*/L^i (with L^i being an erythrocyte bioligand, see Table 3) were examined to study the binding of $V^{IV}O$ species to Hb and the biotransformation in the red blood cells.

Determination of the Binding Constants. The determination of the binding constants for the species $V^{IV}O$–protein and $V^{IV}O$–*carrier*–protein is based on the displacement reaction of the coordinated ligands.[14b,26]

For $(VO)_x$Hb with x = 2,3, analogously to what happens for $(VO)_x$HSA with x = 5,6,[27] the results indicate that the affinities of the sites toward $V^{IV}O^{2+}$ ion are very similar, and, therefore, only a mean value for the binding constant can be calculated. Using the same procedure and notation reported by Kiss and co-workers[7,13c] (explained in detail also in ref 14b), the value of log β can be referred only to the species (VO)Hb:

$$VO^{2+} + Hb \rightleftarrows (VO)Hb \quad (1)$$

The value of log β can be determined through the reaction of displacement between Hb and hTf:

$$(VO)hTf + Hb \rightleftarrows (VO)Hb + hTf \quad (2)$$

From reaction 2, it results that:

$$\log \beta((VO)Hb) = \log \beta_1((VO)hTf) + \log \frac{[(VO)Hb][hTf]}{[(VO)hTf][Hb]} = \log \beta_1((VO)hTf) + \log K_D \quad (3)$$

where K_D indicates the constant for the displacement reaction. The concentrations of (VO)hTf and (VO)Hb can be determined through the double integration of the first-derivative EPR from the parallel resonances M_I = 5/2, 7/2, whereas those of hTf and Hb are from simple stoichiometric considerations.[14b]

The same procedure applies to the calculation of log β of the mixed species *cis*-$VO(ma)_2$(Hb) and *cis*-$VO(dhp)_2$(Hb). As an example, we report here the procedure used for the ternary complex of dhp, where log β refers to the reaction:

$$VO^{2+} + 2dhp + Hb \rightleftarrows (VO)(dhp)_2(Hb) \quad (4)$$

The value of log β is evaluated from the following displacement reaction:

$$VO(dhp)_2(H_2O) + Hb \rightleftarrows (VO)(dhp)_2(Hb) + H_2O \quad (5)$$

$$\log \beta(VO(dhp)_2(Hb)) = \log \beta_2(VO(dhp)_2) + \log \frac{[VO(dhp)_2(Hb)]}{[VO(dhp)_2][Hb]} = \log \beta_2(VO(dhp)_2) + \log K_D \quad (6)$$

In eq 6, log β_2 for $[VO(dhp)_2]$ is known (22.83),[28] the concentrations of $VO(dhp)_2$(Hb) and $[VO(dhp)_2]$ can be obtained measuring the intensities of their M_I = 5/2, 7/2 EPR resonances (see Figure 5) after the double integration of the first-derivative spectrum, and that of Hb from stoichiometry.

Experiments with Red Blood Cells. The experiments with red blood cells were carried out according to the procedures established in the literature.[22,29] Blood was obtained following informed consent from healthy adults and was kept into tubes containing EDTA. EDTA was added to the whole blood and acts as an anticoagulant forming soluble complexes with Ca^{2+} ions; since the plasma, containing the soluble Ca–EDTA complex, was separated and discarded and the red blood cells were washed three times with PBS solution containing glucose (1.4×10^{-1} M NaCl, 5.0×10^{-3} M NaH_2PO_4, 1.1×10^{-2} M glucose; pH 7.40) before the incubation with vanadium solutions, the interaction between EDTA and the V species can be ruled out.

Blood samples were immediately centrifuged for 10 min at 3000 rpm, and the plasma and buffy coat were removed and discarded. The erythrocytes were resuspended in an equal volume of PBS containing 1.1×10^{-2} M glucose to ensure that the hematocrit value was maintained. The erythrocyte suspensions were washed with PBS and centrifuged three times.

The isolated erythrocytes were resuspended in PBS containing glucose (see above) and were incubated at 37 °C and at pH 7.40 with solutions containing vanadium(V) or $[VO(ma)_2]$, $[VO(dhp)_2]$, and $[VO(acac)_2]$ to obtain a final V concentration in the extracellular medium of 9.1×10^{-4} M. Aliquots were taken at different time points (1, 2, and 3 h) and centrifuged for 10 min at 3000 rpm to separate the solution from the erythrocytes. The erythrocytes were washed three times with PBS, transferred into quartz tubes, frozen at 120 K, and the EPR spectra were recorded. Even if the freezing produces erythrocyte lysates, the measured EPR spectra coincide with those of intact red blood cells. On the extracellular medium, the quantitative spectrophotometric determination of V was carried out (see below).

Determination of Vanadium in the Extracellular Medium. To establish the amount of vanadium that crosses the erythrocyte membrane, the V concentration in the extracellular medium was determined. A selective and sensitive spectrophotometric determination of total vanadium in an aqueous solution is based on the reaction with 4-(2-pyridylazo)-resorcinol (PAR).[30] The limit of detection of the method is 0.0028 μg/mL.[31] PAR (L) forms with vanadium(V) an anionic complex $[V^VO_2L]^-$ in the pH range 4.5–8.0 with an absorption maximum at λ_{max} = 542 nm and $\varepsilon_{max} = (3.6–3.7) \times 10^4$ L mol^{-1} cm^{-1}.[32] In slightly acidic or neutral solution and at high temperatures, vanadium(IV) is oxidized very quickly by atmospheric oxygen; therefore, at the conditions used in the experiments (pH 7.4 and 37 °C), the oxidation of V^{IV} to V^V is rapid and quantitative, and the determination of total V can be carried out measuring the absorbance at 542 nm. This was verified carrying out calibration curves for V^V and $[VO(ma)_2]$.

Spectroscopic Measurements. EPR spectra were recorded with an X-band (9.4 GHz) Bruker EMX spectrometer equipped with a HP 53150A microwave frequency counter. Anisotropic spectra were recorded on frozen solutions at 120 K. The addition of DMSO was not necessary, and no improvement in the resolution of the spectra was obtained. When the samples were transferred into the EPR tubes, the spectra were immediately measured. To increase the signal-to-noise ratio, signal averaging was used.[33] As usual for the analysis of the EPR spectra,[34] in all of the figures reported in this Article, only the high field region is shown, the part more sensitive to the identity and

dx.doi.org/10.1021/ic402366x | *Inorg. Chem.* 2014, 53, 1449–1464

Table 1. Possible Coordination Modes and EPR Parameters for Hemoglobin Sites[a]

coordination[b]	A_x^{calcd}[c]	A_y^{calcd}[c]	A_z^{calcd}[c]	A_z^{exptl}	dev.[d]
$COO^-_{Glu/Asp}$, H_2O, H_2O, H_2O	−74.6	−74.3	−176.1	−170.1[e]	3.5
$COO^-_{Glu/Asp}$, H_2O, H_2O, H_2O, H_2O^{ax}	−71.8	−70.3	−171.4	−170.1[e]	0.8
$COO^-_{Glu/Asp}$, $COO^-_{Glu/Asp}$, H_2O, H_2O	−63.2	−60.1	−165.5	−170.1[e]	−2.7
N_{His}(∥), $COO^-_{Glu/Asp}$, H_2O, H_2O	−68.0	−64.1	−167.8	−166.8[f]	0.6
N_{His}(⊥), $COO^-_{Glu/Asp}$, H_2O, H_2O	−68.4	−65.6	−169.0	−166.8[f]	1.3
N_{His}(∥), $COO^-_{Glu/Asp}$, $COO^-_{Glu/Asp}$, H_2O	−59.4	−57.0	−161.7	−166.8[f]	−3.1
N_{His}(⊥), $COO^-_{Glu/Asp}$, $COO^-_{Glu/Asp}$, H_2O	−59.6	−56.1	−159.8	−166.8[f]	−4.2
N_{His}(∥), N_{His}(⊥), $COO^-_{Glu/Asp}$, H_2O	−64.2	−60.8	−164.9	−163.3[g]	1.0
N_{His}(∥), N_{His}(∥), $COO^-_{Glu/Asp}$, H_2O	−60.2	−57.4	−162.0	−163.3[g]	−0.8
N_{His}(∥), N_{His}(⊥), $COO^-_{Glu/Asp}$, $COO^-_{Glu/Asp}$	−55.8	−54.8	−158.9	−163.3[g]	−2.7
N_{His}(∥), N_{His}(∥), $COO^-_{Glu/Asp}$, $COO^-_{Glu/Asp}$	−52.7	−52.1	−156.6	−163.3[g]	−4.1

[a]All values are in 10^{-4} cm^{-1}. [b]In bold are indicated the more likely coordination modes. [c]Calculated with Gaussian software at the level of theory BHandHLYP/6-311g(d,p). [d]Percent deviation from the experimental value calculated as $100 \times (|A_z|^{calcd} - |A_z|^{exptl})/|A_z|^{exptl}$. [e]Site α (g_z = 1.949). [f]Site β (g_z = 1.952). [g]Site γ (g_z = 1.953).

to the amount of the several species in solution. Spectrophotometric measurements were carried out with a Perkin-Elmer Lambda 35 spectrophotometer, and the absorption maximum of $[V^VO_2L]^-$ was read at λ_{max} = 542 nm.

DFT Calculations. The coordination environment of $V^{IV}O^{2+}$ ion bound to Hb was described performing DFT simulations with Gaussian 09 (revision C.01) software.[35] The metal sites of the vanadium in Hb were simulated using 1-methylimidazole for histidine nitrogen (N_{His}) and acetate for carboxylate group of glutamate and aspartate ($COO^-_{Glu/Asp}$). The symbols (∥) and (⊥) indicate a parallel (10° in the calculations) and perpendicular (70° in the calculations) of the imidazole ring of histidine with respect to the V═O bond. The interaction of *cis*-$[VO(ma)_2(H_2O)]$ and *cis*-$[VO(dhp)_2(H_2O)]$ with His-N and Cys-S^- was modeled using 1-MeIm and Ac-Cys-$NHCH_3$, respectively.

All of the structures were optimized in water with the hybrid exchange-correlation functional B3LYP,[36] and a general basis set obtained using 6-311g for V, C, H, N, and O and 6-311+g(d) for S atoms. This choice ensures a good degree of accuracy in the prediction of the structures of first-row transition metal complexes,[37] and in particular of vanadium compounds.[38] The solvent (H_2O) effect was simulated within the framework of the polarizable continuum model (PCM),[39] whose performance was well established in the literature.[38,40,41] For all of the structures, minima were verified through frequency calculations.

The ^{51}V ***A*** tensor was calculated using the functional BHandHLYP (as incorporated in Gaussian) and 6-311g(d,p) basis set with Gaussian 09,[35] or using the functional PBE0[42] and VTZ basis set with ORCA software,[43] according to the procedures previously published.[40b,41,44] It must be taken into account that for a $V^{IV}O^{2+}$ species, the A_z value is usually negative, but in the literature its absolute value is often reported. The theory background was described in detail in refs 44d and 44e. The percent deviation from the absolute experimental value was calculated as: $100 \times (|A_z|^{calcd} - |A_z|^{exptl})/|A_z|^{exptl}$ (see Tables 1 and 2).

RESULTS AND DISCUSSION

Interaction of the $V^{IV}O^{2+}$ Ion with Hemoglobin. The choice of studying the system $V^{IV}O^{2+}$/hemoglobin was due to the high concentration of hemoglobin (even if restricted to the erythrocyes) in the blood, 330 g/L,[23] if compared to that of hTf (1.8−2.7 g/L),[23] HSA (35−50 g/L),[23] and IgG (7.7−20 g/L).[45] The study was carried out on the basis of our previous experience about the interaction between $V^{IV}O^{2+}$ ion and the blood serum proteins, such as transferrin, albumin, and immunoglobulin G.[14,33]

Most of the experimental evidence in the literature indicates that inside the erythrocytes, $V^{IV}O^{2+}$ is bound mainly to hemoglobin.[21,22] As a preliminary step, the EPR spectrum of Hb has been recorded to verify if the signals due to Fe^{2+} may cover or interfere with those of $V^{IV}O^{2+}$ (Figure S1 of the Supporting Information). As pointed out in the Experimental and Computational Section, the percent saturation of the iron sites is about 95%. EPR spectra recorded on frozen solutions containing $V^{IV}O^{2+}$ and Hb revealed that hemoglobin is able to coordinate this metal ion (Supporting Information Figure S1, trace b). It can be observed that the signal due to Fe^{2+} is present only in the low field region (270−310 mT) and does not interfere with the resonances of the first z component of the anisotropic spectrum of $V^{IV}O^{2+}$ ion (M_I = −7/2).

Anisotropic EPR spectra with $V^{IV}O^{2+}$/Hb molar ratios between 1/1 and 8/1 were recorded. In Figure S2 of the Supporting Information, the intensity of the EPR signals at physiological pH of the last two parallel bands (M_I = 5/2 and 7/2) is reported as a function of this ratio. It emerges that the highest intensity of the EPR signals is obtained when the concentration of $V^{IV}O^{2+}$ is twice that of hemoglobin (2/1 ratio). This would suggest that two or three sites are available for the metal coordination.

The high field region of the EPR spectra of the binary system $V^{IV}O^{2+}$/Hb recorded at pH 7.4 with different molar ratios is reported in Figure S3 of the Supporting Information.

From an examination of the EPR spectra in Supporting Information Figure S3, it can be deduced that there are at least two different types of signals, depending on the $V^{IV}O^{2+}$/Hb ratio. The M_I = 7/2 resonance appears to be large and asymmetric and can account for the presence of at least two $V^{IV}O^{2+}$ species with different coordination mode and A_z of 166.8 and 163.3 × 10^{-4} cm^{-1} (Table 1). However, it cannot be excluded that, under the large band centered around 408 mT, there are resonances belonging to other sites; therefore, in analogy to what was recently reported for albumin,[33] the stoichiometry of the binary complex $V^{IV}O^{2+}$−Hb will be indicated with $(VO)_xHb$, x = 2−3. We named the two sites detectable by EPR at pH 7.4 β and γ. By a comparison of the four spectra reported in Supporting Information Figure S3, it can be argued also that, by increasing the metal to ligand ratio, the M_I = 7/2 resonances are subjected to a slight shift toward higher magnetic field values, suggesting the presence of a set of weaker donor atoms. The spectral parameters are reported in Table 1. On the basis of the values of the ^{51}V hyperfine coupling constant on the z axis (A_z), the coordination of $V^{IV}O^{2+}$ in the specific iron sites, that is, the heme groups, can be

dx.doi.org/10.1021/ic402366x | Inorg. Chem. 2014, 53, 1449−1464

excluded because it would give rise to a spectrum with a characteristic A_z value in the range (154−159) × 10^{-4} cm^{-1}.[46]

Once the optimal metal to ligand ratio was determined (characterized by the most intense EPR signal), the EPR spectra with molar ratio 2/1 were measured at different pH values (Figure 1).

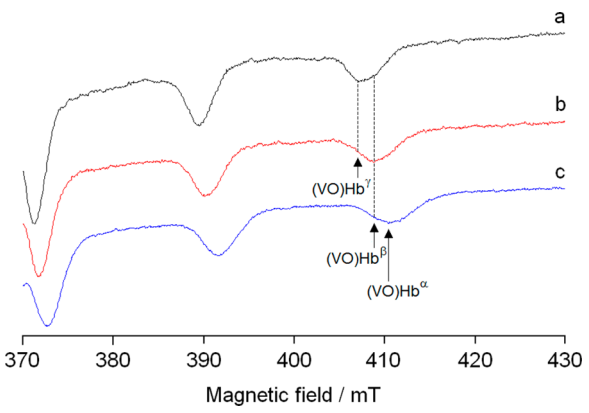

Figure 1. High field region of the X-band anisotropic EPR spectra recorded as a function of pH on frozen solutions (120 K) containing $V^{IV}O^{2+}$/Hb with the 2/1 ratio and $V^{IV}O^{2+}$ 6.2 × 10^{-4} M: (a) pH 7.40; (b) pH 6.30; and (c) pH 5.00. With the dotted lines the M_I = 7/2 resonances of the three coordination sites α, β, and γ (denoted with (VO)Hb$^{\alpha}$, (VO)Hb$^{\beta}$, and (VO)Hb$^{\gamma}$) are indicated.

From the analysis of the spectra, a shift at lower magnetic fields of the M_I = 7/2 resonances with increasing pH value is evident. This means that $V^{IV}O^{2+}$ is coordinated by stronger donor atoms at physiological than at acidic pH and that such donors undergo protonation when the pH is lowered at values <5. An amino acid residue possibly involved in the metal binding is histidine, whose pK_a value of ca. 6 is only slightly lowered when the coordination of His-N is monodentate; for example, Chasteen and co-workers observed the resonances of site B of carboxypeptidase A (only Glu-72 coordinated) at pH < 5 and those of site A (Glu-72, His-69, and His-196 coordinated) at pH > 5, in agreement with what is reported in Figure 1.[47] For hemoglobin, the site occupied at pH 5 is named α, and in it, probably, the His-N are partly protonated and the coordination is due to less basic donors such as the carboxylate groups of aspartate and glutamate residues; however, at this pH value, the imidazole nitrogens of histidines start to undergo deprotonation and contribute to the $V^{IV}O^{2+}$ coordination (shoulder at low-field of the M_I = 7/2 resonance of site α, see trace c of Figure 1). With increasing pH, the site α transforms into β and γ (see above) after the deprotonation of His-N, and the resonances of both of these sites are observed at pH 7.4 (Figure 1, trace a). The change in the relative spectral intensity from pH 6.3 to 7.4 (cf., traces a and b of Figure 1) suggests that in the site γ the number of His-N bound to $V^{IV}O^{2+}$ may be larger than that in the site β.

It is possible to advance plausible hypotheses about the donor atoms coordinated to vanadium by using DFT calculations on $V^{IV}O^{2+}$ model complexes. This approach consists of the comparison of the experimental anisotropic ^{51}V hyperfine coupling constant (A_z^{exptl}) with that of a model species (A_z^{calcd}) calculated by DFT methods (see "DFT calculations" in the Experimental and Computational Section) and has been recently applied with excellent results to the study of the chemical environment of $V^{IV}O^{2+}$ ion in several V proteins.[41] Using the functional BHandHLYP and the basis set 6-311g(d,p), it is possible to calculate the A_z value for a $V^{IV}O^{2+}$ complex with an average deviation from the experimental value lower than 3%.[44a,e] Moreover, if the optimization is performed in water, simulating the effect of the solvent with the polarizable continuum model (PCM), the prediction of A_z is further improved.[41] The results of DFT calculations are reported in Table 1.

The examination of the data in Table 1 allows us to advance the following hypotheses. (i) For the site α, observed at pH 5.0, the most likely coordination mode seems to be that of a COO^- group of glutamate or aspartate with three water molecules in equatorial position and one axial (Figure 2a). At such a pH value, all of the carboxylic groups of Glu and Asp should be in the deprotonated form, being characterized by a low pK_a. This coordination mode has been postulated for sites B of V-carboxypeptidase[47] and V-insulin.[48] (ii) At pH higher than 5, the deprotonation of a first His residue that replaces a water molecule yields the resonances attributable to the $V^{IV}O^{2+}$ coordination in the site β (Figure 2b). In the literature, it has been shown that the orientation of the imidazole ring relative to the V═O double bond (parallel (∥) or perpendicular (⊥)) influences the A_z value.[44b,49] Therefore, both possibilities were examined. From the data in Table 1, it is impossible to establish which of the two options is more likely, even if the complex with a parallel orientation of the imidazole ring gives a slightly better agreement (0.6 vs 1.3% in comparison with the experimental value). Moreover, the parallel arrangement is more stable than the perpendicular one in the absence of any significant interaction with the other residues of the polypeptide chain. (iii) Finally, the further decrease of the A_z value, at physiological pH, could be explained with the coordination of a second His residue, which would replace another water molecule (site γ). Also, in this case, different combinations regarding the orientation of the imidazole rings relative to the V═O bond were considered. The models that give A_z values closer to the experimental one are those with the

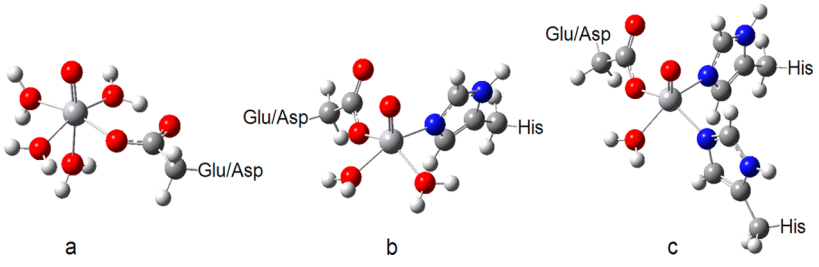

Figure 2. Optimized structures with DFT methods of the sites α (a), β (b), and γ (c) of hemoglobin. In all of the cases, the $V^{IV}O^{2+}$ binding to the protein residues is stabilized by a network of hydrogen bonds.

dx.doi.org/10.1021/ic402366x | Inorg. Chem. 2014, 53, 1449−1464

two imidazole rings parallel to V=O (Figure 2c) and with one ring parallel and another perpendicular.

From these data, it can be concluded that $V^{IV}O^{2+}$ ion is not bound by hemoglobin at the iron specific coordination sites, that is, the heme groups, that there is no exchange between the iron bound to the heme groups and the vanadium added, and that no relevant redox reactions between these two ions are observed. It is noteworthy that the $V^{IV}O^{2+}$ coordination sphere can be studied despite the presence of iron bound to hemoglobin. The environment of the sites β and γ of Hb is similar to that of vanadium in the sites A of V-carboxypeptidase[47] and V-insulin,[48] in the low and high pH forms of V-carbonic anhydrase,[50] in the multimetal binding site (MBS) of V-albumin,[13c,33] and in the unspecific sites of immunoglobulin G.[14c]

The Ternary System $V^{IV}O^{2+}$, Hemoglobin, and Apo-transferrin. The system $V^{IV}O^{2+}$/hTf was widely studied.[13a,b,25a,26,33,51] In this work, the behavior of the ternary $V^{IV}O^{2+}$/Hb/hTf system at molar ratio 2/1/1 and 2/2/1 was examined. The high field region of the EPR spectra recorded at the physiological conditions is reported in Figure 3.

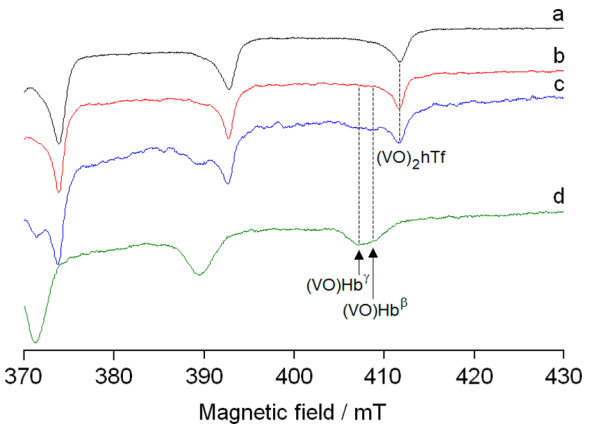

Figure 3. High field region of the X-band anisotropic EPR spectra recorded on frozen solutions (120 K) containing various $V^{IV}O^{2+}$/Hb/hTf molar ratios: (a) 2/0/1 ($V^{IV}O^{2+}$ 5×10^{-4} M, hTf 2.5×10^{-4} M); (b) 2/1/1 ($V^{IV}O^{2+}$ 5×10^{-4} M, Hb 2.5×10^{-4} M, hTf 2.5×10^{-4} M); (c) 2/2/1 ($V^{IV}O^{2+}$ 3.1×10^{-4} M, Hb 3.1×10^{-4} M, hTf 1.55×10^{-4} M); and (d) 2/1/0 ($V^{IV}O^{2+}$ 6.2×10^{-4} M, Hb 3.1×10^{-4} M). With the dotted lines the $M_I = 7/2$ resonances of (VO)$_2$hTf and of the sites β and γ of Hb ((VO)Hb$^{\beta}$ and (VO)Hb$^{\gamma}$) are indicated.

In the system with ratio 2/1/1, apo-transferrin is, in principle, able to bind all vanadium present in solution in the coordination sites of Fe^{3+}, forming (VO)$_2$hTf. As a consequence of the high thermodynamic stability of this complex, almost all of the $V^{IV}O^{2+}$ ion binds to hTf (Figure 3b). The larger stability of hTf than Hb species depends on the fact the two binding sites of transferrin are specific for the metal ions,[2Sb,52] whereas hemoglobin (except heme groups occupied by Fe^{2+}) has only unspecific sites.

With increasing amount of Hb with respect to hTf, the percentage of $V^{IV}O^{2+}$ bound to Hb increases significantly (Figure 3c). It must be noticed that at pH 7.4 both of the sites β and γ are occupied; this means that the thermodynamic stability of the two sites is similar. From these data, knowing the values of log β for the binary species of $V^{IV}O^{2+}$ formed by hTf,[12,14b] the mean value of the binding constant of (VO)$_x$Hb is (see reactions 1 and 2 and eq 3 in "Determination of the Binding Constants" in the Experimental and Computational Section):

$$\log \beta((VO)Hb) = 10.4 \pm 1.0 \quad (7)$$

The obtained value is comparable with that of immunoglobulin G (log β((VO)IgG = 10.3),[14c] and is one order of magnitude larger than that of albumin (log β((VO)HSA = 9.1).[14b]

The Ternary Systems $V^{IV}O^{2+}$, Hemoglobin, and Organic *carrier* (*carrier* = Maltol, 1,2-Dimethyl-3-hydroxy-4(1*H*)-pyridinone, Acetylacetone). In the binary system $V^{IV}O^{2+}$/maltol with molar ratio 1/2, only the complex *cis*-[VO(ma)$_2$(H$_2$O)] exists at pH 7.4 (Figure 4d).[53] The

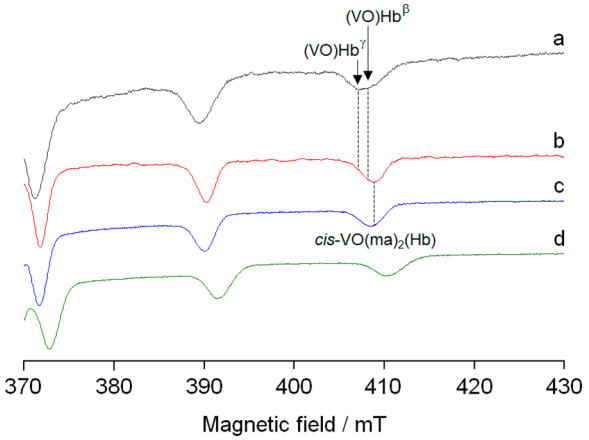

Figure 4. High field region of the X-band anisotropic EPR spectra recorded on frozen solutions (120 K) containing: (a) $V^{IV}O^{2+}$/Hb 2/1 ($V^{IV}O^{2+}$ 6.2×10^{-4} M, Hb 3.1×10^{-4} M); (b) $V^{IV}O^{2+}$/Hb/Hma 2/1/4 ($V^{IV}O^{2+}$ 6.2×10^{-4} M, Hb 3.1×10^{-4} M, Hma 1.24×10^{-3} M); (c) $V^{IV}O^{2+}$/Hma/1-MeIm 1/2/4 ($V^{IV}O^{2+}$ 1.0×10^{-3} M, Hma 2.0×10^{-3} M, 1-MeIm 4.0×10^{-3} M); and (d) $V^{IV}O^{2+}$/Hma 1/2 ($V^{IV}O^{2+}$ 1.0×10^{-3} M, Hma 2.0×10^{-3} M). With the dotted lines the $M_I = 7/2$ resonances of *cis*-VO(ma)$_2$(Hb) and of the sites β and γ of Hb ((VO)Hb$^{\beta}$ and (VO)Hb$^{\gamma}$) are indicated.

anisotropic EPR spectrum recorded in the ternary system containing $V^{IV}O^{2+}$, Hb, and maltol at physiological pH shows the presence of a species in high concentration and a small amount of (VO)$_x$Hb (Figure 4b). The spectral parameters of the main compound (g_z = 1.947 and A_z = 165.4×10^{-4} cm^{-1}) are comparable with those of the ternary complex formed in the system $V^{IV}O^{2+}$, maltol, 1-methylimidazole (1-MeIm), *cis*-[VO(ma)$_2$(1-MeIm)] (g_z = 1.948 and A_z = 164.8×10^{-4} cm^{-1}),[14d,e] for which a *cis*-octahedral coordination with an equatorial position occupied by the nitrogen donor of 1-MeIm was demonstrated through spectroscopic, potentiometric, and DFT results.[14d,e] Therefore, the EPR resonances observed in the system with hemoglobin can be attributed to a mixed complex *cis*-VO(ma)$_2$(Hb), characterized by an equatorial–equatorial and equatorial–axial arrangement of the two maltolate ligands and coordination of hemoglobin in the fourth equatorial position through a His-N of the polypeptide chain (Scheme 2).

The double integration of the first-derivative spectrum allowed us to find the approximate percent amounts of *cis*-VO(ma)$_2$(Hb) (~95%) and (VO)$_x$Hb (~5%). With these data, using the procedure discussed in "Determination of the Binding Constants" in the Experimental and Computational Section, log β for VO(ma)$_2$(Hb) is:

dx.doi.org/10.1021/ic402366x | Inorg. Chem. 2014, 53, 1449–1464

Scheme 2. Mixed Complexes Formed by Hemoglobin: (a) *cis*-VO(ma)$_2$(Hb) and (b) *cis*-VO(dhp)$_2$(Hb)

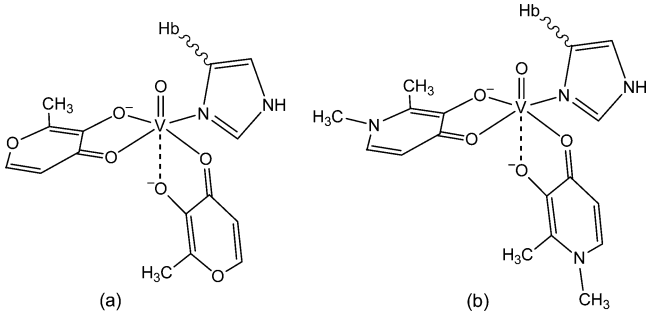

$$\log \beta(\mathrm{VO(ma)_2(Hb)}) = 19.6 \pm 1.2 \quad (8)$$

The value of 19.6 for log β of VO(ma)$_2$(Hb) appears to be plausible and comparable with those of *cis*-VO(ma)$_2$(hTf), *cis*-VO(ma)$_2$(HSA), and *cis*-VO(ma)$_2$(IgG), which are in the range 19.2−19.6.[14d]

In Table 2, the comparison between the values of A_z calculated by DFT methods for *cis*-[VO(ma)$_2$(1-MeIm)] and the experimental ones of the mixed species *cis*-VO(ma)$_2$(Protein) formed by hTf, HSA, IgG, and Hb is reported. It must be noticed that the agreement is rather good, even if the data of the simulations confirm the tendency of DFT calculations to underestimate slightly A_z.

The potentiometric data indicate that, between pH 5 and 8, in the binary system $V^{IV}O^{2+}$/Hdhp the bis-chelated complex is the main species in aqueous solution. It is present in the two forms [VO(dhp)$_2$], square pyramidal, and *cis*-[VO(dhp)$_2$(H$_2$O)], distorted octahedral.[28,54] The anisotropic EPR spectrum recorded in the ternary system with $V^{IV}O^{2+}$, Hb, and Hdhp in aqueous solution at pH 7.4 shows the presence of a species not detected in the systems $V^{IV}O^{2+}$/Hb and VO^{2+}/Hdhp (cf., traces a, b and f of Figure 5). The value of A_z (162.7 × 10^{-4} cm^{-1}) is intermediate between that of *cis*-[VO(dhp)$_2$(H$_2$O)] (166.2 × 10^{-4} cm^{-1}) and [VO(dhp)$_2$] (157.4 × 10^{-4} cm^{-1}),[28,54] and this indicates that the equatorial water molecule in the *cis*-octahedral species is replaced by a stronger donor. A_z is practically coincident with that of *cis*-[VO(dhp)$_2$(1-MeIm)] (163.0 × 10^{-4} cm^{-1}), whose existence was demonstrated in the literature.[14a,b] Therefore, the stoichiometry *cis*-VO(dhp)$_2$(Hb) is attributed to this mixed complex (Scheme 2).

From an examination of Figure 5, it is evident that by using a low Hdhp/Hb molar ratio (traces b and f), only the resonances of the ternary species *cis*-VO(dhp)$_2$(Hb) are observable, whereas at higher ratio (trace d) the enlargement of the resonances indicates the presence of the binary complexes of Hdhp.

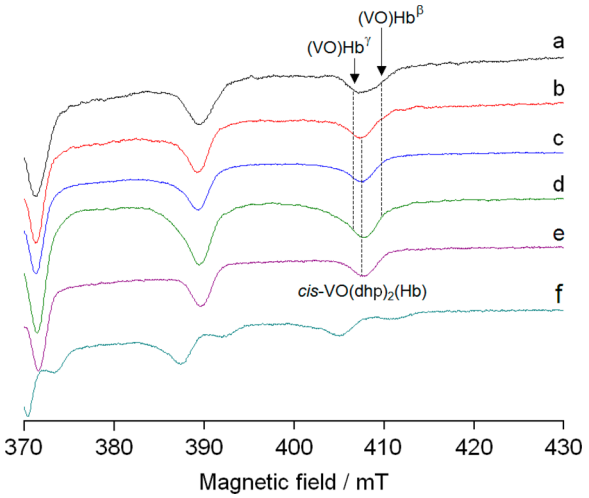

Figure 5. High field region of the X-band anisotropic EPR spectra recorded on frozen solutions (120 K) containing: (a) $V^{IV}O^{2+}$/Hb 2/1 ($V^{IV}O^{2+}$ 6.2 × 10^{-4} M, Hb 3.1 × 10^{-4} M); (b) $V^{IV}O^{2+}$/Hb/Hdhp 2/1/4 ($V^{IV}O^{2+}$ 6.2 × 10^{-4} M, Hb 3.1 × 10^{-4} M, Hdhp 1.24 × 10^{-3} M); (c) $V^{IV}O^{2+}$/Hb/Hdhp 4/1/8 ($V^{IV}O^{2+}$ 1.0 × 10^{-3} M, Hb 2.5 × 10^{-4} M, Hdhp 2.0 × 10^{-3} M); (d) $V^{IV}O^{2+}$/Hb/Hdhp 8/1/16 ($V^{IV}O^{2+}$ 1.0 × 10^{-3} M, Hb 1.25 × 10^{-4} M, Hdhp 2.0 × 10^{-3} M); (e) $V^{IV}O^{2+}$/Hdhp/1-MeIm 1/2/4 ($V^{IV}O^{2+}$ 1.0 × 10^{-3} M, Hdhp 2.0 × 10^{-3} M, 1-MeIm 4.0 × 10^{-3} M); and (f) $V^{IV}O^{2+}$/Hdhp 1/2 ($V^{IV}O^{2+}$ 1.0 × 10^{-3} M, Hdhp 2.0 × 10^{-3} M). With the dotted lines the M_I = 7/2 resonances of *cis*-VO(dhp)$_2$(Hb) and of the sites β and γ of Hb ((VO)Hb$^{\beta}$ and (VO)Hb$^{\gamma}$) are indicated.

The behavior of the system $V^{IV}O^{2+}$/Hb/Hdhp is comparable with that of $V^{IV}O^{2+}$/hTf/Hdhp, $V^{IV}O^{2+}$/HSA/Hdhp, and $V^{IV}O^{2+}$/IgG/Hdhp, where the formation of *cis*-VO(dhp)$_2$(hTf), *cis*-VO(dhp)$_2$(HSA), and *cis*-VO(dhp)$_2$(IgG) was proved.[14a,c] In such species, an imidazole nitrogen of an accessible His residue replaces the water molecule in *cis*-[VO(dhp)$_2$(H$_2$O)] and occupies the fourth equatorial coordination position. Therefore, EPR spectra can be interpreted on the basis of a mixture formed by *cis*-[VO(dhp)$_2$(H$_2$O)] and [VO(dhp)$_2$], on one hand, and *cis*-VO(dhp)$_2$(Hb), on the other (see trace b of Figure S4 of the Supporting Information); in particular, the spectrum recorded in the system $V^{IV}O^{2+}$/Hb/Hdhp with molar ratio 8/1/16 can be reproduced considering 69% of $V^{IV}O^{2+}$ as *cis*-VO(dhp)$_2$(Hb) and 31% as *cis*-[VO(dhp)$_2$(H$_2$O)] and [VO(dhp)$_2$]. Such data allow us to obtain an estimate of the value of log β for *cis*-VO(dhp)$_2$(Hb):

Table 2. ^{51}V Hyperfine Coupling Constants Calculated by DFT Methods for $V^{IV}O$ Species Formed by Histidine and Cysteine Models (1-MeIm and Ac-Cys-NHCH$_3$) and Comparison with the Mixed Species Formed by $V^{IV}O^{2+}$, Hma, or Hdhp (*carrier*) and the Blood Proteins[a]

Complex	A_z^{calcd}[b]	A_z^{calcd}[c]	A_z^{exptl}	A_z(hTf)[d]	A_z(HSA)[e]	A_z(IgG)[f]	A_z(Hb)[g]	Dev.[h]	Dev.[i]
cis-[VO(ma)$_2$(1-MeIm)]	−162.6	−161.2	−164.8	−164.7	−165.5	−164.6	−165.4	−1.3	−2.2
cis-[VO(dhp)$_2$(1-MeIm)]	−160.7	−158.9	−163.0	−163.3	−162.1	−162.6	−162.7	−1.4	−2.5
cis-[VO(ma)$_2$(Ac-Cys-NHCH$_3$)]$^-$	−158.3	−154.6	−158.1					+0.1	−2.2

[a]Values reported in 10^{-4} cm^{-1}. [b]A_z calculated with Gaussian software at the level of theory BHandHLYP/6-311g(d,p). [c]A_z calculated with ORCA software at the level of theory PBE0/VTZ. [d]A_z for *cis*-VO(*carrier*)$_2$(hTf). [e]A_z for *cis*-VO(*carrier*)$_2$(HSA). [f]A_z for *cis*-VO(*carrier*)$_2$(IgG). [g]A_z for *cis*-VO(*carrier*)$_2$(Hb). [h]Percent deviation of A_z calculated with Gaussian from the experimental values for *cis*-[VO(*carrier*)$_2$(1-MeIm)] or *cis*-[VO(ma)$_2$(Cys-S$^-$)]$^-$ (see Figure 10) expressed as 100 × ($|A_z|^{calcd} - |A_z|^{exptl}$)/$|A_z|^{exptl}$. [i]Percent deviation of A_z calculated with ORCA from the experimental value for *cis*-[VO(*carrier*)$_2$(1-MeIm)] or *cis*-[VO(ma)$_2$(Cys-S$^-$)]$^-$ (see Figure 10) expressed as 100 × ($|A_z|^{calcd} - |A_z|^{exptl}$)/$|A_z|^{exptl}$.

dx.doi.org/10.1021/ic402366x | Inorg. Chem. 2014, 53, 1449−1464

$$\log \beta(\mathrm{VO(dhp)_2(Hb)}) = 25.8 \pm 1.0 \quad (9)$$

The value of log β for $VO(dhp)_2(Hb)$ has been determined with a procedure analogous to that used in the case of maltol (see above). It is similar to those of $VO(dhp)_2$(hTf) (25.5), $VO(dhp)_2$(IgG) (25.6), and $VO(dhp)_2$(HSA) (25.9).[14b,c] The higher concentration of $VO(dhp)_2(Hb)$ in the ternary system with Hb with respect to that measured at the same experimental conditions in the systems containing hTf, HSA, and IgG must be related to the higher number of surface histidines of Hb (26^{55}) than hTf (12^{56}), IgG (12^{57}), and HSA (6^{58}).

DFT calculations allowed us to confirm these hypotheses. They showed that the value of A_z expected for *cis*-$[VO(dhp)_2(1\text{-MeIm})]$ (160.7×10^{-4} cm^{-1}) is very similar to that of *cis*-$VO(dhp)_2(Hb)$ (162.7×10^{-4} cm^{-1}) (Table 2). The simulations also suggested that, in the absence of any significant interaction with other groups of the protein, the aromatic ring of imidazole should be parallel to the V=O direction.

Potentiometric and spectroscopic studies indicate that in the system $V^{IV}O^{2+}$/Hacac, around the physiological pH, $V^{IV}O^{2+}$ ion is present as neutral complex $[VO(acac)_2]$ with very low hydrolysis degree.[59,60] Figure 6 shows that in the system

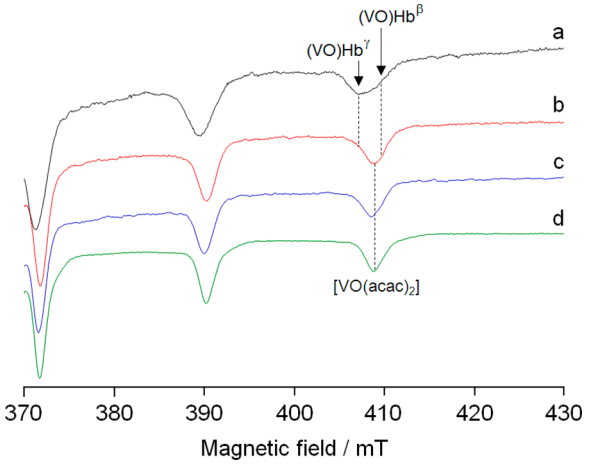

Figure 6. High field region of the X-band anisotropic EPR spectra recorded on frozen solutions (120 K) containing: (a) $V^{IV}O^{2+}$/Hb 2/1 ($V^{IV}O^{2+}$ 6.2×10^{-4} M, Hb 3.1×10^{-4} M); (b) $V^{IV}O^{2+}$/Hb/Hacac 2/1/4 ($V^{IV}O^{2+}$ 6.2×10^{-4} M, Hb 3.1×10^{-4} M, Hacac 1.24×10^{-3} M); (c) $V^{IV}O^{2+}$/Hacac/1-MeIm 1/2/4 (VO^{2+} 1.0×10^{-3} M, Hacac 2.0×10^{-3} M, 1-MeIm 4.0×10^{-3} M); and (d) $V^{IV}O^{2+}$/Hacac 1/2 ($V^{IV}O^{2+}$ 1.0×10^{-3} M, Hacac 2.0×10^{-3} M). With the dotted lines the M_I = 7/2 resonances of $[VO(acac)_2]$ and of the sites β and γ of Hb ((VO)Hb$^{\beta}$ and (VO)Hb$^{\gamma}$) are indicated.

$V^{IV}O^{2+}$/Hb/Hacac, the species $[VO(acac)_2]$ (in high amount) and $(VO)_x$Hb (in low amount) coexist (trace b). The absence of a mixed species VO–Hb–acac can be explained taking into account the geometry of the bis-chelated compound formed by acetylacetonate, square pyramidal rather than *cis*-octahedral (see Scheme 1), which hinders the coordination of an accessible His residue on the equatorial plane of $V^{IV}O^{2+}$ ion.[14a] In other words, since $[VO(acac)_2]$ does not possess coordinated water molecules to be replaced, it does not have any tendency to form mixed complexes of the type *cis*-$VO(carrier)_2$(Hb), in contrast with what was previously observed for Hma and Hdhp. The fact that no ternary species is formed by $V^{IV}O^{2+}$, acetylacetonate, and 1-methylmidazole further supports these findings (Figure 6c).

Uptake of Vanadium Compounds by Red Blood Cells. The uptake of the potential antidiabetic $V^{IV}O^{2+}$ compounds by red blood cells was followed by EPR and UV–vis spectroscopy. The behavior of vanadate(V) was re-examined and taken as a reference for the analysis of the other systems. UV–vis spectra allowed us to determine the amount of the total vanadium in the extracellular medium and, indirectly, the percentage of V complex incubated that enters inside the cells.

The interaction of vanadium(V) with the red blood cells was widely studied and discussed in the literature.[16,18,20–22,29,61–64] At pH 7.4, V^V exists as a mixture of mono- (V1), di- (V2), and tetranuclear ions (V4), depending on the total metal concentration in solution.[1b] For our purposes, we will indicate generically with vanadate(V) or V^V these anionic species. Vanadate(V) crosses the cell wall easily and penetrates the membrane much faster than do V^{IV} salts via anion channels.[61] This result can be demonstrated by the inhibition of V^V transport by 4,4′-diisothiocyanostilbene-2,2′-disulfonic acid (DIDS), the specific inhibitor of the anion channels.[16] This mechanism of accumulation of V^V via anion channels has been also demonstrated for ascidians (or sea squirts) in the seawater.[65] Inside the cells, vanadate(V) initially could bind to the phosphate-binding site of (Na,K)-ATPase on the cytoplasmatic side of the membrane.[20] Subsequently, it is reduced to vanadium(IV) by the intact erythrocyte at the expense of cellular glutathione;[22] the presence of the GSH depletor diethyl maleate blocks the process and supports this mechanism.[22,61] When V^{IV} instead of V^V is incubated, a delay in the uptake by red blood cells is observed, and this has been attributed to the time required for the partial oxidation of vanadium(IV) prior to possible uptake.[18,20] The quantitative representation of the uptake of vanadate(V) by erythrocytes as a function of the time at 37 °C is shown in Figure 7. The trend

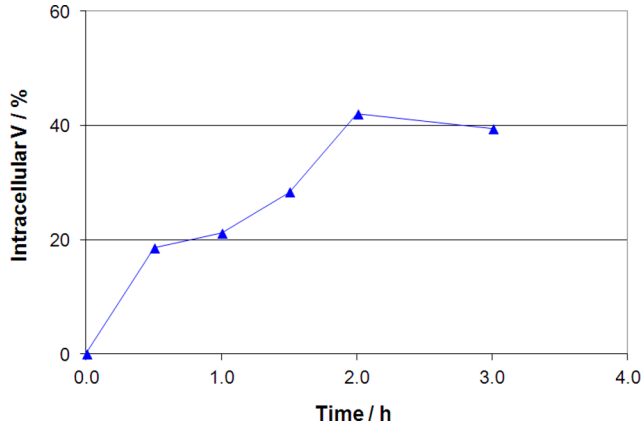

Figure 7. Time dependence of the intracellular V percentage upon incubation with vanadate(V) at 37 °C.

is almost superimposable to that described by Delgado et al.,[29] with an initial increase in the intracellular concentration of V, which reaches a plateau after 120 min. The uptake has been described as a two-step process, the first representing the equilibration across the red blood cell membrane and the second the intracellular reduction of vanadium(V) and its subsequent complexation.[21,22] The reduction is a first-order process with a $t_{1/2}$ of about 130 min,[22] and this is in agreement with our results. From Figure 7, it can be noted that the

dx.doi.org/10.1021/ic402366x | Inorg. Chem. 2014, 53, 1449–1464

maximum amount of V inside the red blood cells corresponds to ca. 40% of V^V incubated.

EPR spectra of the erythrocyte samples incubated with V^V are reported in Figure 8. The spectral intensity increases mainly

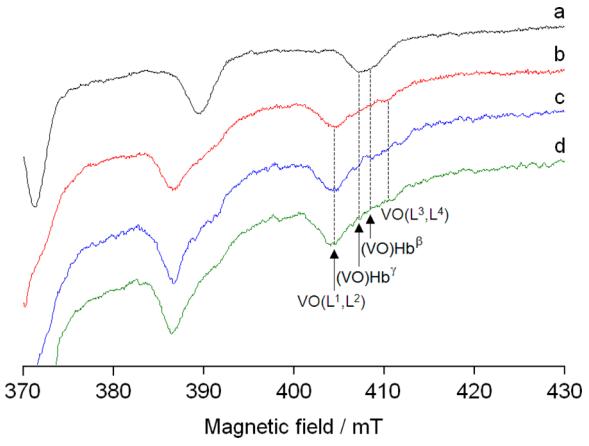

Figure 8. High field region of the X-band anisotropic EPR spectra recorded at 120 K on the systems: (a) $V^{IV}O^{2+}$/Hb 2/1 ($V^{IV}O^{2+}$ 6.2 × 10^{-4} M, Hb 3.1 × 10^{-4} M); (b) lysate samples of erythrocytes incubated with V^V for 1 h; (c) lysate samples of erythrocytes incubated with V^V for 2 h; and (d) lysate samples of erythrocytes incubated with V^V for 3 h. With the dotted lines the M_I = 7/2 resonances of $VO(L^1,L^2)$ and $VO(L^3,L^4)$ and of the sites β and γ of Hb ($(VO)Hb^{\beta}$ and $(VO)Hb^{\gamma}$) are indicated.

in the time range 0−2 h (cf., with Figure 7). The detection of an EPR signal in the red blood cells confirms the reduction of vanadate(V) to $V^{IV}O^{2+}$ observed in the literature.[16,20−22,29,62,63]

EPR resonances of at least four $V^{IV}O^{2+}$ species were detected with absence of any time dependence. A_z values are in the range (160−168) × 10^{-4} cm^{-1}; in the same system, Delgado et al. reported only one species with A_z of 168 × 10^{-4} cm^{-1}.[29] However, until now, no attribution has been attempted in the literature, and no spectroscopic evidence that V^{IV} binds to hemoglobin in vivo was published.[21,22,29,63,64] To try to characterize the identity of the four species observed inside the red blood cells, the composition of the erythrocytes must be taken into account (Table 3).[23,66]

Among the four different species observed, the resonances of the β and γ sites of hemoglobin are revealed; that is, a part of $V^{IV}O^{2+}$ is bound to Hb as binary complexes ($(VO)Hb)^{\beta}$ and $(VO)Hb^{\gamma}$ in Figure 8). Thus, the coordination of Hb to V in the erythrocytes is unambiguously proved. This is in agreement with previous papers, in which it was detected that the amount of $V^{IV}O^{2+}$ bound to hemoglobin can decrease upon addition of adenosine 5′-triphosphate (ATP) and 2,3-diphosphoglycerate, suggesting that intracellular bioligands can compete with Hb for $V^{IV}O^{2+}$ coordination.[22] Concerning the other two species, these are characterized by g_z = 1.946 and A_z = 167.7 × 10^{-4} cm^{-1} and g_z = 1.959 and A_z = 159.6 × 10^{-4} cm^{-1}. These signals cannot be attributed to the binary species of $V^{IV}O^{2+}$ with the intracellular components listed in Table 3. Any attempt to reproduce the two EPR signals using model systems (for example, $V^{IV}O^{2+}$/Hb/GSH, $V^{IV}O^{2+}$/Hb/lact, $V^{IV}O^{2+}$/lact/GSH, $V^{IV}O^{2+}$/GSH/ATP) was unsuccessful; however, the results reported in this study are in line with the observation of De Cremer and co-workers, who carrying out liquid chromatography experiments (size exclusion and ion exchange chromatography) detected three different species in the packed cells, one of them being a VO−Hb complex.[64]

We indicated these two unidentified complexes with $VO(L^1,L^2)$ and $VO(L^3,L^4)$ (see Figure 8), where L^1, L^2, L^3, and L^4 are erythrocyte bioligands, such as proteins or low molecular mass components. The high g_z value for $VO(L^1,L^2)$ (1.959) seems to be characteristic of S coordination to V^{IV}; for example, the $V^{IV}O^{2+}$ species formed by GSH with the interaction of Cys-S^- shows a value of g_z in the range 1.956−1.959.[67] The experiments with human erythrocyte ghosts demonstrated the interaction of V with protein sulfhydryl groups.[68] Therefore, the interaction of $V^{IV}O^{2+}$ with the membrane proteins from the cytoplasmatic side is possible and must be considered in the future. Furthermore, the binding to the membrane proteins has been already proved for decavanadate(V), $V_{10}O_{28}^{6-}$, after its uptake in the cells through the anion channels.[69]

The results obtained with the three potential antidiabetic compounds are shown in Figure 9 and Figure S5 of the Supporting Information. Delgado et al. showed that, when V^{IV} is put in contact with the erythrocytes as a $[VO(carrier)_2]$ compound, the incorporation depends on its stability in aqueous solution.[29] Ten years ago, Yang et al., on the basis of the different inhibition of V^V and $V^{IV}O^{2+}$ complexes by DIDS, concluded that $[VO(ma)_2]$ and $[VO(acac)_2]$ cross the membrane lipid bilayer via simple passive diffusion.[16] The mechanism can be described by two consecutive reversible reactions, the first representing the equilibration of $[VO(carrier)_2]$ species across the red blood cell membrane (kinetic constants κ_1 and κ_{-1}) and the second one its transformation as a result of the subsequent complexation reactions (kinetic constants κ_2 and κ_{-2}). The reversibility of the two steps is a

Table 3. Concentration of the Most Important Bioligands of the Red Blood Cells[a]

bioligand[b,c]	concentration	bioligand[b,c]	concentration
hemoglobin (Hb)	**5.1 mM**	alanine	275 ± 60 μM
adenosine 5′-diphosphate (ADP)	216 ± 36 μM	**aspartate**	**306 ± 81 μM**
adenosine 5′-triphosphate (ATP)	**1.35 ± 0.035 mM**	**glutamate**	**265 ± 89 μM**
glutathione reduced (GSH)	**2.23 ± 0.35 mM**	glutamine	624 ± 136 μM
lactate (lact)	**932 ± 211 μM**	creatine	330 ± 110 μM
inorganic phosphate	480 ± 5 μmol	ergothioneine	355 ± 112 μM
sialic acid	825 ± 28 μM	taurine	349 ± 57 μM
2,3-diphosphoglycerate (2,3-DPG)	4.17 ± 0.64 mM	sorbitol	31.1 ± 5.3 mM
glucose 1,6-diphosphate (GDP)	180−300 μM	urea	4.12 ± 0.42 mM

[a]All of the concentrations were taken from ref 66. [b]The bioligands with concentration higher than 200 μM are shown. [c]The bioligands that may have more affinity toward $V^{IV}O^{2+}$ are indicated in bold.

dx.doi.org/10.1021/ic402366x | Inorg. Chem. 2014, 53, 1449−1464

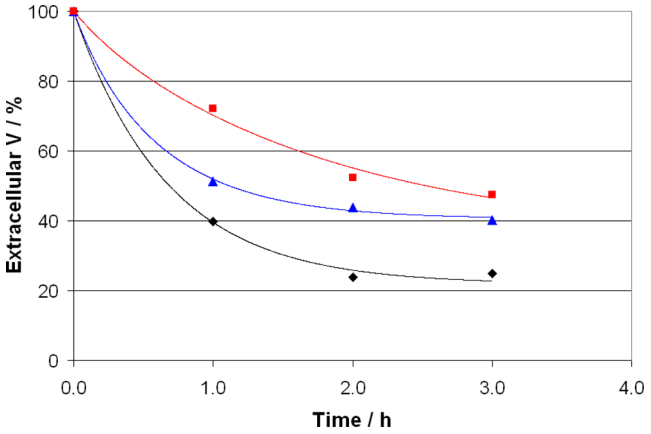

Figure 9. Time dependence of the extracelluar V percentage upon incubation with $[VO(ma)_2]$ (black ◆), $[VO(acac)_2]$ (blue ▲), and $[VO(dhp)_2]$ (red ■) at 37 °C. The experimental points were fitted with the kinetic constants reported in Table 4.

condition necessary to explain the ratio between the concentration of V in the extra- and intracellular medium observed in the experiments; if one of two steps was irreversible, the reactions should be shifted toward one of the two directions, and this would be incompatible with the results obtained in this study and in the literature.[18−20] The whole process can be represented as:

$$V^{IV}O(carrier)_{2,extra} \underset{\kappa_{-1}}{\overset{\kappa_1}{\rightleftharpoons}} V^{IV}O(carrier)_{2,intra} \underset{\kappa_{-2}}{\overset{\kappa_2}{\rightleftharpoons}} V^{IV}O(carrier, L, L')_{intra} \quad (10)$$

where $V^{IV}O(carrier,L,L')$ is the species formed after the partial (systems with maltol and 1,2-dimethyl-3-hydroxy-4(1*H*)-pyridinone, see below) or total (system with acac) displacement of the *carrier* ligand. The concentration of $V^{IV}O(carrier)_{2,extra}$ will be indicated generically as extracellular V (see Figure 9) and the sum of $V^{IV}O(carrier)_{2,intra}$ and $V^{IV}O(carrier,L,L')$ as intracellular V (Figure S5 of the Supporting Information). The value of extra- and intracellular V concentration is a function of the time through the kinetic constants κ_1, κ_{-1}, κ_2, and κ_{-2}.[70] As an example, the percent extracellular V concentration as a function of t follows the equation:[70]

$$\text{intracellular V}/\% = 100 \times \left[\frac{\kappa_{-1}\kappa_{-2}}{\lambda_1\lambda_2} + \frac{\kappa_1(\lambda_1 - \kappa_2 - \kappa_{-2})}{\lambda_1(\lambda_1 - \lambda_2)} e^{-\lambda_1 t} + \right.$$
$$\left. + \frac{\kappa_1(\kappa_2 + \kappa_{-2} - \lambda_2)}{\lambda_2(\lambda_1 - \lambda_2)} e^{-\lambda_2 t} \right] \quad (11)$$

where $\lambda_1 = 1/2(p + q)$, $\lambda_2 = 1/2(p - q)$, $p = (\kappa_1 + \kappa_{-1} + \kappa_2 + \kappa_{-2})$, and $q = [p^2 - 4(\kappa_1\kappa_2 + \kappa_{-1}\kappa_{-2} + \kappa_1\kappa_{-2})]^{1/2}$.[70] The kinetic constants used to fit the experimental points (Figure 9 and Supporting Information Figure S5) are reported in Table 4.

Table 4. Kinetic Constants and Percent Intracellular Concentration at the Equilibrium ($\%V_{eq}$) for the Uptake of $[VO(ma)_2]$, $[VO(dhp)_2]$, and $[VO(acac)_2]$ in the Red Blood Cells

complex	κ_1/h^{-1}	κ_{-1}/h^{-1}	κ_2/h^{-1}	κ_{-2}/h^{-1}	$\%V_{eq}$	R^2
$[VO(ma)_2]$	1.20	0.99	13.45	6.89	77.7	0.992
$[VO(dhp)_2]$	0.48	1.00	2.09	0.73	56.2	0.970
$[VO(acac)_2]$	1.10	1.25	1.79	2.71	59.2	0.996

The values of the intracellular V concentration at the equilibrium ($\%V_{eq}$) are 77.7% for $[VO(ma)_2]$, 56.2% for $[VO(dhp)_2]$, and 59.2% for $[VO(acac)_2]$ and can be interpreted as the percent V concentration in the red blood cells when the equilibrium between the rates of influx and efflux across the cell membrane (see ref 18) and of ligand exchange in the cytosol is reached. The results indicate that a high percentage of the antidiabetic V compound, greater than 50%, enters the red blood cells. However, as it can be observed from an examination of Figures 9, more than 1 h is necessary to reach this amount; during this period, $V^{IV}O$ species can undergo side-reactions, such as redox processes,[13e] which in this study will be in a first approximation neglected. If Figures 7 and S5 of the Supporting Information are compared, it can be observed that the amount of the neutral $V^{IV}O$ complexes that is taken up by erythrocytes by diffusion is higher than that of vanadate(V) that enters through the anion channel; this confirms the results previously reached in the literature.[29]

It is interesting to observe that other essential metal ions, such as cobalt and zinc, are accumulated by red blood cells by simple diffusion through the cellular membrane when ionophores or complexing agents are present.[71] In particular, the uptake of Zn^{2+} ion complexed by ethylmaltolate follows an exponential increase with time, and the diffusion process reaches a steady state in about 90 min,[71a] in line with the results shown in Supporting Information Figure S5.

Even if it has been already proved that neutral V complexes are taken up by erythrocytes through passive diffusion processes,[16,29] no data exist on the transformation of these species upon the interaction with the cell membrane and with cytosol bioligands and on the identity of the species inside the red blood cells. For this reason, EPR spectra were recorded on the lysate samples when the erythrocytes are incubated with $[VO(ma)_2]$, $[VO(dhp)_2]$, and $[VO(acac)_2]$. These are reported in Figures 10−12.

In Figure 10 are shown EPR spectra recorded on the lysate samples of the erythrocytes incubated with $[VO(ma)_2]$. In the

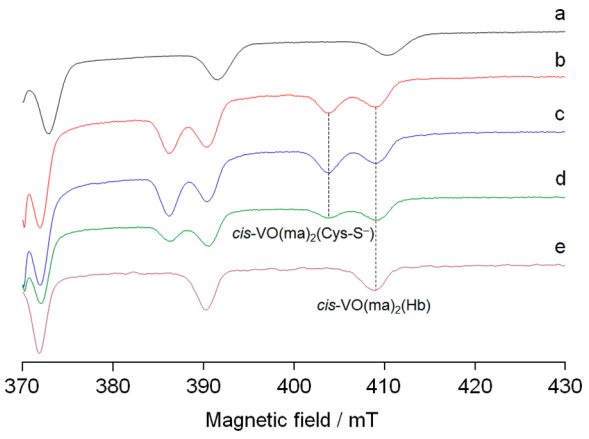

Figure 10. High field region of the X-band anisotropic EPR spectra recorded at 120 K on the systems: (a) $V^{IV}O^{2+}$/Hma 1/2 ($V^{IV}O^{2+}$ 1.0×10^{-3} M, Hma 2.0×10^{-3} M); (b) lysate samples of erythrocytes incubated with $[VO(ma)_2]$ for 1 h; (c) lysate samples of erythrocytes incubated with $[VO(ma)_2]$ for 2 h; (d) lysate samples of erythrocytes incubated with $[VO(ma)_2]$ and hTf for 1 h ($V^{IV}O^{2+}$ 9.1×10^{-4} M, Hma 1.8×10^{-3} M, hTf 4.5×10^{-4} M); and (e) $V^{IV}O^{2+}$/Hb/Hma 2/1/4 ($V^{IV}O^{2+}$ 6.2×10^{-4} M, Hb 3.1×10^{-4} M, Hma 1.24×10^{-3} M). With the dotted lines the $M_I = 7/2$ resonances of *cis*-$VO(ma)_2$(Cys-S$^-$) and *cis*-$VO(ma)_2$(Hb) are indicated.

dx.doi.org/10.1021/ic402366x | *Inorg. Chem.* 2014, 53, 1449−1464

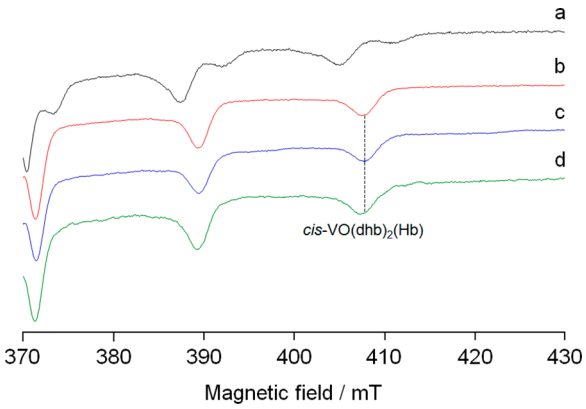

Figure 11. High field region of the X-band anisotropic EPR spectra recorded at 120 K on the systems: (a) $V^{IV}O^{2+}$/Hdhp 1/2 ($V^{IV}O^{2+}$ 1.0 × 10^{-3} M, Hdhp 2.0 × 10^{-3} M); (b) lysate samples of erythrocytes incubated with $[VO(dhp)_2]$ for 1 h; (c) lysate samples of erythrocytes incubated with $[VO(dhp)_2]$ for 2 h; and (d) $V^{IV}O^{2+}$/Hb/Hdhp 2/1/4 ($V^{IV}O^{2+}$ 6.2 × 10^{-4} M, Hb 3.1 × 10^{-4} M, Hdhp 1.24 × 10^{-3} M). With the dotted line the M_I = 7/2 resonance of *cis*-$VO(dhp)_2$(Hb) is indicated.

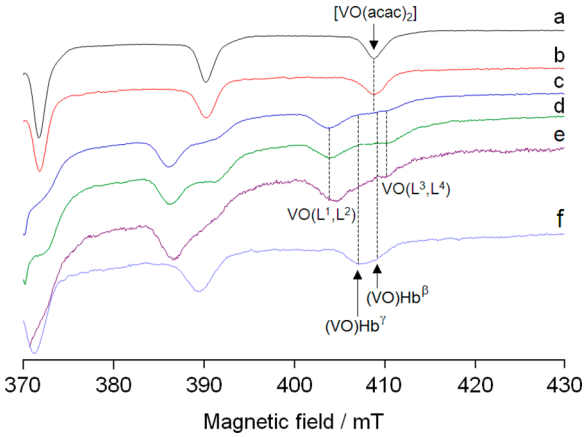

Figure 12. High field region of the X-band anisotropic EPR spectra recorded at 120 K on the systems: (a) $V^{IV}O^{2+}$/Hacac 1/2 ($V^{IV}O^{2+}$ 1.0 × 10^{-3} M, Hacac 2.0 × 10^{-3} M); (b) $V^{IV}O^{2+}$/Hb/Hacac 2/1/4 ($V^{IV}O^{2+}$ 6.2 × 10^{-4} M, Hb 3.1 × 10^{-4} M, Hacac 1.24 × 10^{-3} M); (c) lysate samples of erythrocyte incubated with $[VO(acac)_2]$ for 1 h; (d) lysate samples of erythrocyte incubated with $[VO(acac)_2]$ for 2 h; (e) lysate samples of erythrocyte incubated with V^V for 1 h; and (f) $V^{IV}O^{2+}$/Hb 2/1 ($V^{IV}O^{2+}$ 6.2 × 10^{-4} M, Hb 3.1 × 10^{-4} M). With the dotted lines the M_I = 7/2 resonances of $[VO(acac)_2]$, $VO(L^1,L^2)$, $VO(L^3,L^4)$ and of the two β and γ sites of Hb ($(VO)Hb^{\beta}$ and $(VO)Hb^{\gamma}$) are indicated.

time range 0−3 h, an increase of the spectral intensity was observed in agreement with the trend of Figure S5 of the Supporting Information. Inside the red blood cells two species are formed, one with g_z = 1.947 and A_z = 165.4 × 10^{-4} cm^{-1} and another with g_z = 1.960, A_z = 158.7 × 10^{-4} cm^{-1}. The first is identifiable with the mixed species formed with Hb, *cis*-$VO(ma)_2$(Hb), with the equatorial coordination of a His-N of hemoglobin polypeptide chain to *cis*-$[VO(ma)_2(H_2O)]$ (see Scheme 2). The second one has A_z similar to that of the ternary complex formed by maltolate and GSH (A_z = 159.1 × 10^{-4} cm^{-1}),[67] even if a significant larger value of g_z is measured in this work (1.960 vs 1.949). This may suggest the coordination of a thiolate-S^- donor stemming from GSH of the cytosol or from −SH of the proteins of erythrocyte inner membrane. Therefore, a S^- donor would replace the equatorial water molecule of *cis*-$[VO(ma)_2(H_2O)]$, lowering the A_z and raising g_z value. To further confirm this assumption, the structure of *cis*-$[VO(ma)_2(Ac\text{-}Cys\text{-}NHCH_3)]^-$, where Ac-Cys-$NHCH_3$ is a simple model for the S^- coordination, was optimized using DFT methods (see "DFT calculations" in the Experimental and Computational Section). A_z values were calculated with Gaussian and ORCA and are reported in Table 2. Both softwares satisfactorily predict A_z (with deviations of 0.1 and −2.2%); these data appear to be in line with what was reported in the literature for $V^{IV}O$ compounds with S donors[44e] and allow us to confirm the attribution proposed. This means that neutral *cis*-$[VO(ma)_2(H_2O)]$ species penetrates the cellular membrane, and inside the red blood cells the weak water ligand is replaced by stronger donors, such as His-N of Hb, Cys-S^- of GSH or of a membrane protein, which are present in the erythrocytes at high concentration. The process is described in Scheme 3.

It has been supposed that a low ratio between V in the plasma and erythrocytes may depend on the absence in the experiments of human serum transferrin (hTf), which forms stable species with $V^{IV}O^{2+}$ ion in the serum.[61] To verify this hypothesis, experiments with erythrocytes incubated with $[VO(ma)_2]$ and apo-transferrin for 1 h were carried out (trace d of Figure 10). The results show that there is only a small difference with respect to the measurements without hTf: the decrease of the amount of $[VO(ma)_2]$ absorbed by red blood cells, quantified around 10%, may be due to the oxidation processes of $V^{IV}O$ to V^V favored in the presence of human serum transferrin.[13e] At the end of this experiment too, *cis*-$VO(ma)_2$(Hb) and *cis*-$VO(ma)_2$(Cys-S^-) were observed.

The behavior of $[VO(dhp)_2]$ is simpler than $[VO(ma)_2]$. EPR spectra recorded on the erythrocytes incubated with $[VO(dhp)_2]$ and on some model systems are represented in Figure 11 and are characterized by a slight increase of the spectral intensity as a function of the time. As it can be noticed, the same species revealed in the system with Hb is observed (cf., traces b and d of Figure 11); in other words, *cis*-octahedral complex *cis*-$[VO(dhp)_2(H_2O)]$ enters inside the red blood cells, and an imidazole nitrogen belonging to an accessible His residue of hemoglobin replaces the H_2O molecule in the fourth equatorial position forming *cis*-$VO(dhp)_2$(Hb). Differently from what was observed with Hma, in the system with Hdhp only one species is detected, probably because of the higher stability of the dhp complexes. No traces of the binary complexes of Hb and Hdhp are observed.

In Figure 12 EPR spectra recorded on the erythrocytes incubated with $[VO(acac)_2]$ are reported. In contrast with the systems with Hma and Hdhp, the bis-chelated species does not survive after the interaction with the membrane and the uptake in the cellular environment. Even if the presence of a minor amounts of $[VO(acac)_2]$ cannot be excluded, the spectra are very similar to those detected with vanadate(V) (Figure 8). This means that acetylacetonate ligands are lost and free $V^{IV}O^{2+}$ ion interacts with hemoglobin and unidentified bioligands of the erythrocytes (Scheme 3). The intensity ratio between the resonances of the four species does not change from 0 to 3 h after the incubation. The time dependence of the uptake of $[VO(acac)_2]$ is analogous to that of $[VO(ma)_2]$ and $[VO(dhp)_2]$ (see Figure S5 of the Supporting Information); in this case, the second step of the kinetic mechanism discussed above (governed by constants κ_2 and κ_{-2}) accounts for the displacement of the two acetylacetonato anions, with the

dx.doi.org/10.1021/ic402366x | Inorg. Chem. 2014, 53, 1449−1464

Scheme 3. Interaction of $[VO(ma)_2]$, $[VO(dhp)_2]$, and $[VO(acac)_2]$ with the Red Blood Cell Membrane and Their Transformation into the Cytosol of Erythrocytes[a]

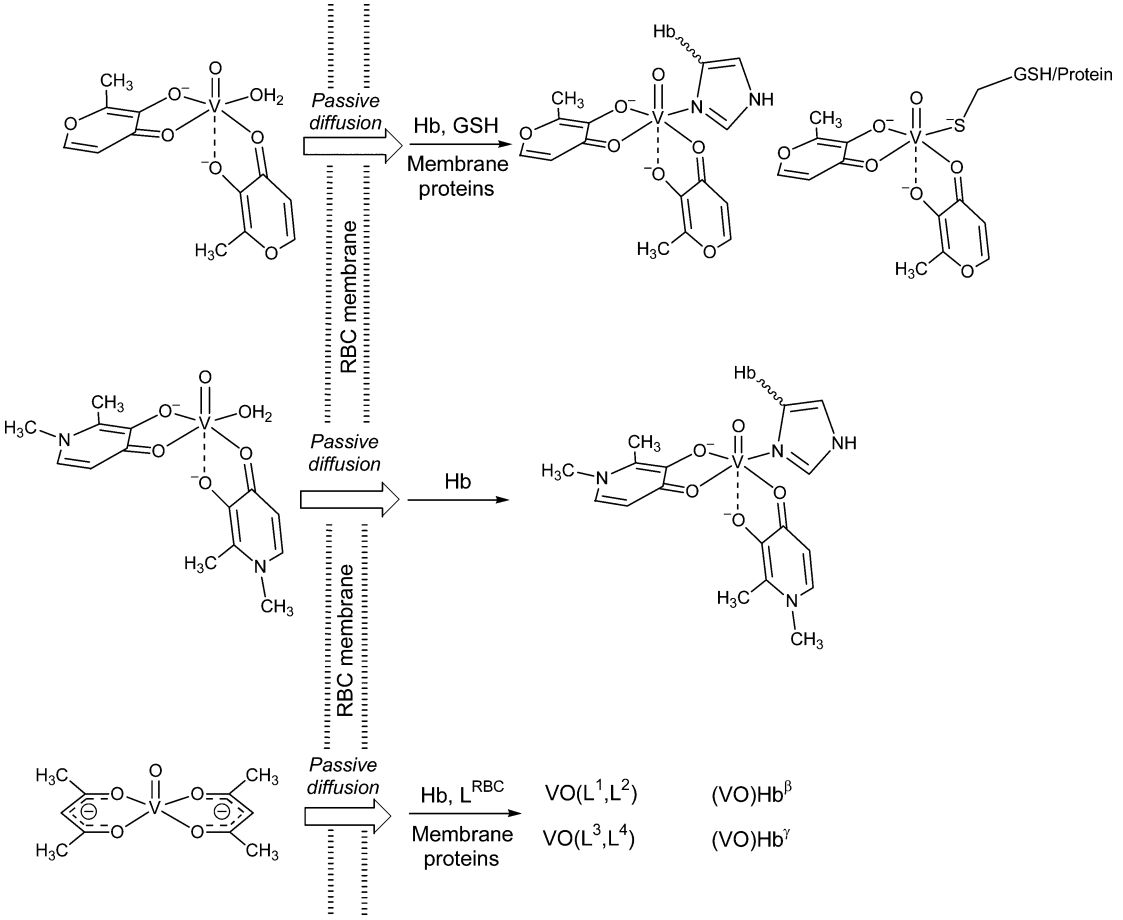

[a]As shown in Scheme 1, $[VO(ma)_2]$ and $[VO(dhp)_2]$ transform in aqueous solution into *cis*-$[VO(ma)_2(H_2O)]$ and *cis*-$[VO(dhp)_2(H_2O)]$.

coordination of the intracellular bioligands following a first-order kinetic. With the kinetic data available in this moment, it appears to be plausible that the loss of acac from $V^{IV}O^{2+}$ takes place when the neutral complex is in the cytosol and bioligands with higher affinity than acetylacetonate bind $V^{IV}O^{2+}$ ion rather than when the insulin-mimetic compound interacts with the erythrocyte membrane (for other species, for example $[V^{V}O_2(dipic)]^-$, the interaction with the cellular membrane affects the biotransformation and, possibly, the effects of the V compounds[72]).

During the recent past, the different activity of the potential antidiabetic VOL_2 compounds was put in relationship with the structural features, the absorption in the gastrointestinal tract, the biotransformation in the blood serum, and the interaction with the cell membrane. The fact that hTf displaces the original *carrier* and most of $V^{IV}O^{2+}$ is transported as (VO)hTf/$(VO)_2$hTf seems to be incompatible with the significant difference in the antidiabetic activity of V compounds and induces one to think that the pharmacologically active species may partially retain their identity and that the form of transport may be variable. Often, however, the possibility that a consistent part of V compounds may enter inside the red blood cells is not specifically considered when their transport in the blood toward the targets in the organism is studied.

More than 15 years ago, Sabbioni and co-workers examined the literature values for vanadium concentration in the serum and blood; the analysis of the results revealed that, in most of the cases, different amounts of V were found with values slightly larger in the blood than in the serum.[73] These data found a confirmation in other papers, where it is reported that the V concentration in the blood can reach 10 times that in the serum.[74] This suggests that a distribution of vanadium between the serum and erythrocytes can occur and that a part of vanadium absorbed in the intestine and entered in the bloodstream is taken up by the red blood cells. Recently, Crans and Willsky groups attempted to correlate the antidiabetic activity with total concentration of V in the serum; the results revealed that, although V accumulation in serum was dose-dependent, no correlation between total serum V concentration and the insulin-enhancing response can be determined. On the basis of these data, the authors suggested that V pools other than the total serum are likely related to the antidiabetic effect of this metal.[75]

The results presented in this study indicate that the interaction with the red blood cells cannot be neglected and that V compounds distribute between the erythrocytes and plasma with a ratio depending on the *carrier* ligand, the thermodynamic stability, and, presumably, the structural features of the complex (square pyramidal or *cis*-octahedral geometry). For the well-known potential antidiabetic drugs $[VO(ma)_2]$, $[VO(dhp)_2]$, and $[VO(acac)_2]$, a percent amount larger than 50% is found inside the red blood cell, and such a

dx.doi.org/10.1021/ic402366x | *Inorg. Chem.* 2014, 53, 1449−1464

Table 5. Predicted Percent Distribution of the $V^{IV}O$ Species Formed from the Biotransformation of $[VO(ma)_2]$, $[VO(dhp)_2]$, and $[VO(acac)_2]$ in Red Blood Cells[a]

species[b]	$[VO(ma)_2]$			$[VO(dhp)_2]$			$[VO(acac)_2]$		
	10 μM	100 μM	**700 μM**	10 μM	100 μM	**500 μM**	10 μM	100 μM	**500 μM**
$VO(carrier)_2$(Hb)	8.7	62.0	**88.1**	87.2	96.5	**98.1**			
$(VO)_x$Hb[c]	90.9	37.6	**11.6**	12.1	2.7	**1.1**	99.7	98.7	**83.5**
$[VO(carrier)_2]$	0.1	0.2	**0.3**	0.7	0.8	**0.8**	0.0	1.0	**16.2**
$[VO(ATPH_{-1})_2]^{8-}$	0.2	0.1	**0.0**	0.0	0.0	**0.0**	0.1	0.1	**0.1**
$[VO(lactH_{-1})_2]^{2-}$	0.1	0.1	**0.0**	0.0	0.0	**0.0**	0.1	0.1	**0.1**

[a]In bold are the results obtained for the concentration observed during the experiments carried out in this study (Figures 10–12). [b]*Carrier* is ma, dhp, or acac. [c]As mentioned in the text, only a mean value for log β of $(VO)_x$Hb can be calculated, and this is referred to the species (VO)Hb (see eq 7).

value reaches 70–80% for $[VO(ma)_2]$. Once these compounds are taken up in the erythrocytes, different biotransformation processes are observed that can be connected with the pharmacological activity. In particular, the transformations in the red blood cells are mainly determined by the thermodynamic stability of the $V^{IV}O$ species and by the geometry assumed in the aqueous solution at the physiological conditions. When the *carrier* is not particularly strong, the bioligands of the cell, such as hemoglobin, other proteins, and low molecular mass components, can displace it, and the complexation scheme follows that displayed by V^V, with the interaction of reduced $V^{IV}O^{2+}$ ion with Hb and other (undetermined) ligands; this is what was found for $[VO(acac)_2]$. When the ligand forms *cis*-octahedral complexes (Hma and Hdhp), the fourth equatorial site can be occupied by a His-N of hemoglobin forming *cis*-$VO(carrier)_2$(Hb) (and also by a Cys-S^- in the case of maltolate).

An attempt to describe the biotransformation processes of $[VO(ma)_2]$, $[VO(dhp)_2]$, and $[VO(acac)_2]$ in the red blood cells can be carried out using the stability constants for (VO)Hb, *cis*-$VO(ma)_2$(Hb), *cis*-$VO(dhp)_2$(Hb) species found in this work and those of the binary and ternary complexes formed by the most important components of the blood cells (Hb, ATP, GSH, lactate, aspartate, and glutamate, in bold in Table 3). The values of log β were taken from the literature.[28,53,59,67,76] In Table 5 are summarized the percent amounts of the species formed after the biotransformation of $[VO(ma)_2]$, $[VO(dhp)_2]$, and $[VO(acac)_2]$, when the concentration of the V drug is in the range necessary to observe insulin-enhancing effects (10–100 μM[1b,77–79]) and the concentration of the bioligands is that in the red blood cells. The prediction for the system containing $[VO(dhp)_2]$ reflects very well the experimental results (Figure 11). For $[VO(ma)_2]$, the main species expected is *cis*-$VO(ma)_2$(Hb), in agreement with the spectral measurements (Figure 10); however, the secondary species should be $(VO)_x$Hb and not $[VO(ma)_2(GSH)]^{2-}$, whose stability constant is known (27.7[67]). Therefore, it is likely that in *cis*-$VO(ma)_2$(Cys-S^-) the coordination involves a Cys-S^- stemming from a membrane protein rather than from intracellular GSH. For $[VO(acac)_2]$, $(VO)_x$Hb and $[VO(acac)_2]$ are expected, but only the first species is experimentally observed in high amount; therefore, the future challenge is to characterize the structure and the thermodynamic stability constants of $VO(L^1,L^2)$ and $VO(L^3,L^4)$, see Figure 12. It must also be noticed that, with decreasing the V concentration, the percentage of $(VO)_x$Hb should increase significantly and that it should be probably the main species formed under the physiological conditions when the *carrier* has an intermediate strength (maltol, acetylacetone); only with strong *carriers*, such as Hdhp, *cis*-$VO(carrier)_2$(Hb) may be the main species in the red blood cells also at V concentration close to 10 μM.

CONCLUSIONS

The results of this study demonstrate that hemoglobin binds $V^{IV}O^{2+}$ ion at physiological pH in at least two sites of comparable strength named β and γ, forming a species $(VO)_x$Hb with $x = 2-3$. It is plausible that, in line with what was reported for serum proteins such as HSA and IgG, such sites are not specific for $V^{IV}O^{2+}$ and involve (as suggested by DFT methods) His-N and/or Glu/Asp-COO^- donors. The value of the stability constant for (VO)Hb (log β = 10.4) is significantly lower than that for hTf (log β_1 = 13.0); this is due to the coordination of $V^{IV}O^{2+}$ to the iron-specific sites in apotransferrin. Log β for (VO)Hb is comparable with that of IgG (log β = 10.3) and is higher than that measured for HSA (log β = 9.1). Therefore, the strength order of the blood proteins for $V^{IV}O^{2+}$ ion is hTf $\gg$ Hb $\approx$ IgG > HSA.

The ternary systems containing hemoglobin and three potential antidiabetic compounds formed by maltol, 1,2-dimethyl-3-hydroxy-4(1*H*)-pyridinone, and acetylacetone, $[VO(ma)_2]$, $[VO(dhp)_2]$, and $[VO(acac)_2]$, show analogies with what was published for the corresponding systems with hTf, HSA, and IgG.[14a–d] In particular, at physiological pH, *cis*-octahedral complexes in which Hb binds $V^{IV}O^{2+}$ through an imidazole nitrogen of an accessible His residue, are formed. For *cis*-$VO(ma)_2$(Hb) and *cis*-$VO(dhp)_2$(Hb), log β values of 19.6 and 25.8 are measured, comparable with those of the analogous species of apo-transferrin, albumin, and immunoglobulin G, *cis*-$VO(carrier)_2$(hTf), *cis*-$VO(carrier)_2$(HSA), and *cis*-$VO(carrier)_2$(IgG), where *carrier* is ma or dhp. No formation of ternary species is observed in the system with Hacac; this may be explained, in agreement with what was reported in the literature,[14a] with the geometry in solution of $[VO(acac)_2]$, square pyramidal, that hinders the equatorial coordination of the protein donors.

The experiments of uptake of $[VO(ma)_2]$, $[VO(dhp)_2]$, and $[VO(acac)_2]$ by the red blood cells confirm that these neutral compounds penetrate the erythrocyte membrane through passive diffusion. Percent amounts higher than 50% are found in the intracellular medium. Some of the $V^{IV}O^{2+}$ species formed inside the red blood cells were characterized. $[VO(dhp)_2]$ transforms quantitatively in *cis*-$VO(dhp)_2$(Hb); $[VO(ma)_2]$ in *cis*-$VO(ma)_2$(Hb) and in *cis*-$VO(ma)_2$(Cys-S^-) with the equatorial coordination of a thiolate S^- stemming from GSH or, most probably, from a membrane protein; and finally $[VO(acac)_2]$ yields $(VO)_x$Hb and two unidentified complexes $VO(L^1,L^2)$ and $VO(L^3,L^4)$, where L^1, L^2, L^3, and L^4 are red

dx.doi.org/10.1021/ic402366x | *Inorg. Chem.* 2014, 53, 1449–1464

blood cell bioligands such as membrane or cytosol (for example, Hb) proteins and/or low molecular mass components. Interestingly, the same species $(VO)_x$Hb, $VO(L^1,L^2)$, and $VO(L^3,L^4)$ are detected in the system with vanadate(V), demonstrating that for $[VO(acac)_2]$ the interaction with intracellular bioligands of the cytosol stronger than acac results in a loss of the two anionic ligands.

The results of this study indicate that the interaction with the red blood cells cannot be neglected when the transport or the pharmacological action of a V compound is considered and that a distribution between the erythrocytes and plasma is achieved. The ratio of such a distribution depends on the strength of the *carrier* ligand and the structural features of the complex at physiological conditions (square pyramidal or *cis*-octahedral geometry). These results are in agreement with the analytical determinations of V in the biological fluids, characterized by larger values in the blood than in the serum.[73] Recent data also suggest that V pools other than the total serum are likely related to the antidiabetic action of the vanadium complexes.[75]

As a consequence of the uptake by the red blood cells, a significant fraction of $V^{IV}O$ complexes is transported in the blood by erythrocytes and in this form reaches the target organs. On the other hand, the biotransformation in the cytosol can partly or totally deactivate the specific $V^{IV}O^{2+}$ drug. This must be taken into account in the future in the studies concerning the transport and the action of the pharmacologically active V compounds. The fate of the potential antidiabetic compounds, once they entered and transformed inside the erythrocytes, is not predictable. In fact, it is not known if these compounds can, under the appropriate conditions, be excreted by the erythrocytes and carry out their pharmacological effects, or remain confined in an inactive form until the death of the red blood cells. In the first case, the erythrocytes would only contribute to the transport of the antidiabetic compounds in the blood, whereas in the second one they would act as a reservoir to store these compounds in an inactive form. Because the different effectiveness of the V antidiabetic compounds depends on the amount reaching the target organs, the importance to establish their distribution between blood serum and erythrocytes is evident.

Finally, it must be observed that the processes discussed in this work, in particular the biodistribution between the plasma and the erythrocytes and the subsequent biotransformation in the red blood cells with the possible interaction with hemoglobin, should be considered for all of the metal drugs and the pharmacologically active coordination compounds.

■ ASSOCIATED CONTENT

Ⓢ Supporting Information

Figures with EPR spectra and intensity, and time dependence of the intracellular V percentage. This material is available free of charge via the Internet at http://pubs.acs.org.

■ AUTHOR INFORMATION

Corresponding Author

*E-mail: garribba@uniss.it.

Notes

The authors declare no competing financial interest.

■ ACKNOWLEDGMENTS

We thank Dr. Monica Pirastru, Prof. Bruno Masala, and Prof. Laura Manca (Dipartimento di Scienze Biomediche, and Centro Interdisciplinare per lo Sviluppo della Ricerca Biotecnologica e per lo Studio della Biodiversità della Sardegna, Università di Sassari) for providing the blood samples used in this study and Prof. Mauro Rustici (Dipartimento di Chimica e Farmacia, Università di Sassari) for his valuable suggestions concerning the interpretation of the kinetic data.

■ REFERENCES

(1) (a) Crans, D. C.; Smee, J. J.; Gaidamauskas, E.; Yang, L. *Chem. Rev.* **2004**, *104*, 849−902. (b) Rehder, D. *Bioinorganic Vanadium Chemistry*; John Wiley & Sons Ltd.: Chichester, 2008.

(2) (a) Rehder, D. *Future Med. Chem.* **2012**, *4*, 1823−1837. (b) Costa Pessoa, J.; Tomaz, I. *Curr. Med. Chem.* **2010**, *17*, 3701−3738.

(3) (a) Thompson, K. H.; Orvig, C. *Coord. Chem. Rev.* **2001**, *219*−*221*, 1033−1053. (b) Shechter, Y.; Goldwaser, I.; Mironchik, M.; Fridkin, M.; Gefel, D. *Coord. Chem. Rev.* **2003**, *237*, 3−11. (c) Sakurai, H.; Yoshikawa, Y.; Yasui, H. *Chem. Soc. Rev.* **2008**, *37*, 2383−2392.

(4) Thompson, K. H.; Orvig, C. *J. Inorg. Biochem.* **2006**, *100*, 1925−1935.

(5) (a) Thompson, K. H.; McNeill, J. H.; Orvig, C. *Chem. Rev.* **1999**, *99*, 2561−2572. (b) Thompson, K. H.; Liboiron Barry, D.; Hanson Graeme, R.; Orvig, C. In *Medicinal Inorganic Chemistry*; Sessler, J. L., Doctrow, S. R., McMurry, T. J., Lippard, S. J., Eds.; American Chemical Society: Washington, DC, 2005; Vol. *903*, pp 384−399. (c) Thompson, K. H.; Orvig, C. In *Metal Ions in Biological Systems*; Sigel, H., Sigel, A., Eds.; Marcel Dekker: New York, 2004; Vol. *41*, pp 221−252.

(6) Thompson, K. H.; Lichter, J.; LeBel, C.; Scaife, M. C.; McNeill, J. H.; Orvig, C. *J. Inorg. Biochem.* **2009**, *103*, 554−558.

(7) Kiss, T.; Jakusch, T.; Hollender, D.; Dörnyei, A. In *Vanadium: The Versatile Metal*; Kustin, K., Costa Pessoa, J., Crans, D. C., Eds.; American Chemical Society: Washington, DC, 2007; Vol. *974*, pp 323−339.

(8) Kiss, T.; Jakusch, T.; Hollender, D.; Dornyei, A.; Enyedy, E. A.; Costa Pessoa, J.; Sakurai, H.; Sanz-Medel, A. *Coord. Chem. Rev.* **2008**, *252*, 1153−1162.

(9) Jakusch, T.; Costa Pessoa, J.; Kiss, T. *Coord. Chem. Rev.* **2011**, *255*, 2218−2226.

(10) Kiss, T.; Jakusch, T.; Gyurcsik, B.; Lakatos, A.; Enyedy, É. A.; Sija, É. *Coord. Chem. Rev.* **2012**, *256*, 125−132.

(11) Sanna, D.; Micera, G.; Garribba, E. *Inorg. Chem.* **2009**, *48*, 5747−5757.

(12) Jakusch, T.; Hollender, D.; Enyedy, E. A.; Gonzalez, C. S.; Montes-Bayon, M.; Sanz-Medel, A.; Costa Pessoa, J.; Tomaz, I.; Kiss, T. *Dalton Trans.* **2009**, 2428−2437.

(13) (a) Willsky, G. R.; Goldfine, A. B.; Kostyniak, P. J.; McNeill, J. H.; Yang, L. Q.; Khan, H. R.; Crans, D. C. *J. Inorg. Biochem.* **2001**, *85*, 33−42. (b) Liboiron, B. D.; Thompson, K. H.; Hanson, G. R.; Lam, E.; Aebischer, N.; Orvig, C. *J. Am. Chem. Soc.* **2005**, *127*, 5104−5115. (c) Correia, I.; Jakusch, T.; Cobbinna, E.; Mehtab, S.; Tomaz, I.; Nagy, N. V.; Rockenbauer, A.; Costa Pessoa, J.; Kiss, T. *Dalton Trans.* **2012**, *41*, 6477−6487. (d) Mehtab, S.; Gonçalves, G.; Roy, S.; Tomaz, A. I.; Santos-Silva, T.; Santos, M. F. A.; Romão, M. J.; Jakusch, T.; Kiss, T.; Costa Pessoa, J. *J. Inorg. Biochem.* **2013**, *121*, 187−195. (e) Gonçalves, G.; Tomaz, A. I.; Correia, I.; Veiros, L. F.; Castro, M. M. C. A.; Avecilla, F.; Palacio, L.; Maestro, M.; Kiss, T.; Jakusch, T.; Garcia, M. H. V.; Costa Pessoa, J. *Dalton Trans.* **2013**, *42*, 11841−11861.

(14) (a) Sanna, D.; Micera, G.; Garribba, E. *Inorg. Chem.* **2010**, *49*, 174−187. (b) Sanna, D.; Buglyó, P.; Micera, G.; Garribba, E. *J. Biol. Inorg. Chem.* **2010**, *15*, 825−839. (c) Sanna, D.; Micera, G.; Garribba, E. *Inorg. Chem.* **2011**, *50*, 3717−3728. (d) Sanna, D.; Biro, L.; Buglyo, P.; Micera, G.; Garribba, E. *Metallomics* **2012**, *4*, 33−36. (e) Sanna, D.; Bíró, L.; Buglyó, P.; Micera, G.; Garribba, E. *J. Inorg. Biochem.* **2012**, *115*, 87−99. (f) Sanna, D.; Ugone, V.; Micera, G.; Garribba, E. *Dalton Trans.* **2012**, *41*, 7304−7318. (g) Sanna, D.; Micera, G.; Garribba, E. *Inorg. Chem.* **2013**, *52*, 11975−11985.

(15) Ghio, A. J.; Piantadosi, C. A.; Wang, X.; Dailey, L. A.; Stonehuerner, J. D.; Madden, M. C.; Yang, F.; Dolan, K. G.; Garrick, M. D.; Garrick, L. M. *Am. J. Physiol.* **2005**, *289*, L460−L467.
(16) Yang, X.; Wang, K.; Lu, J.; Crans, D. C. *Coord. Chem. Rev.* **2003**, *237*, 103−111.
(17) (a) Nielsen, F. H. In *Metal Ions in Biological Systems*; Sigel, H., Sigel, A., Eds.; Marcel Dekker: New York, 1995; Vol. *31*, pp 543−573. (b) Nielsen, F. H. In *Vanadium Compounds. Chemistry, Biochemistry, and Therapeutic Applications*; Tracey, A. S., Crans, D. C., Eds.; American Chemical Society: Washington, DC, 1998; Vol. *711*, pp 297−307.
(18) Harris, W. R.; Friedman, S. B.; Silberman, D. *J. Inorg. Biochem.* **1984**, *20*, 157−169.
(19) (a) Sabbioni, E.; Marafante, E.; Amantini, L.; Ubertalli, L.; Birattari, C. *Bioinorg. Chem.* **1978**, *8*, 503−515. (b) De Cremer, K. In *Handbook of Elemental Speciation II − Species in the Environment, Food, Medicine & Occupational Health*; Cornelis, R., Crews, H., Caruso, J., Heumann, K. G., Eds.; John Wiley & Sons Ltd.: Chichester, 2005; pp 464−487.
(20) Heinz, A.; Rubinson, K. A.; Grantham, J. J. *J. Lab. Clin. Med.* **1982**, *100*, 593−612.
(21) Cantley, L. C.; Aisen, P. *J. Biol. Chem.* **1979**, *254*, 1781−1784.
(22) Macara, I. G.; Kustin, K.; Cantley, L. C., Jr. *Biochim. Biophys. Acta, Gen. Subj.* **1980**, *629*, 95−106.
(23) Schaller, J.; Gerber, S.; Kämpfer, U.; Lejon, S.; Trachsel, C. *Human Blood Plasma Proteins: Structure and Function*; John Wiley & Sons Ltd.: Chichester, 2008.
(24) Nagypál, I.; Fábián, I. *Inorg. Chim. Acta* **1982**, *61*, 109−113.
(25) (a) Chasteen, D. N. *Coord. Chem. Rev.* **1977**, *22*, 1−36. (b) Sun, H.; Cox, M.; Li, H.; Sadler, P. *Struct. Bonding (Berlin)* **1997**, *88*, 71−102.
(26) Kiss, T.; Jakusch, T.; Bouhsina, S.; Sakurai, H.; Enyedy, É. A. *Eur. J. Inorg. Chem.* **2006**, 3607−3613.
(27) Chasteen, N. D.; Francavilla, J. *J. Phys. Chem.* **1976**, *80*, 867−871.
(28) Buglyo, P.; Kiss, T.; Kiss, E.; Sanna, D.; Garribba, E.; Micera, G. *J. Chem. Soc., Dalton Trans.* **2002**, 2275−2282.
(29) Delgado, T. C.; Tomaz, A. I.; Correia, I.; Costa Pessoa, J.; Jones, J. G.; Geraldes, C. F. G. C.; Castro, M. M. C. A. *J. Inorg. Biochem.* **2005**, *99*, 2328−2339.
(30) Taylor, M. J. C.; van Staden, J. F. *Analyst* **1994**, *119*, 1263−1276.
(31) He, X.; Tubino, M.; Rossi, A. V. *Anal. Chim. Acta* **1999**, *389*, 275−280.
(32) Genç, F.; Gavazov, K.; Türkyilmaz, M. *Cent. Eur. J. Chem.* **2010**, *8*, 461−467.
(33) Sanna, D.; Garribba, E.; Micera, G. *J. Inorg. Biochem.* **2009**, *103*, 648−655.
(34) Kiss, T.; Jakusch, T.; Costa Pessoa, J.; Tomaz, I. *Coord. Chem. Rev.* **2003**, *237*, 123−133.
(35) Frisch, M. J.; Trucks, G. W.; Schlegel, H. B.; Scuseria, G. E.; Robb, M. A.; Cheeseman, J. R.; Scalmani, G.; Barone, V.; Mennucci, B.; Petersson, G. A.; Nakatsuji, H.; Caricato, M. L. X.; Hratchian, H. P.; Izmaylov, A. F.; Bloino, J.; Zheng, G.; Sonnenberg, J. L.; Hada, M.; Ehara, M.; Toyota, K.; Fukuda, R.; Hasegawa, J.; Ishida, M.; Nakajima, T.; Honda, Y.; Kitao, O.; Nakai, H.; Vreven, T.; Montgomery, J. A., Jr.; Peralta, J. E.; Ogliaro, F.; Bearpark, M.; Heyd, J. J.; Brothers, E.; Kudin, K. N.; Staroverov, V. N.; Keith, T.; Kobayashi, R.; Normand, J.; Raghavachari, K.; Rendell, A.; Burant, J. C.; Iyengar, S. S.; Tomasi, J.; Cossi, M.; Rega, N.; Millam, J. M.; Klene, M.; Knox, J. E.; Cross, J. B.; Bakken, V.; Adamo, C. J. J.; Gomperts, R.; Stratmann, R. E.; Yazyev, O.; Austin, A. J.; Cammi, R.; Pomelli, C.; Ochterski, J. W.; Martin, R. L.; Morokuma, K.; Zakrzewski, V. G.; Voth, G. A.; Salvador, P.; Dannenberg, J. J.; Dapprich, S.; Daniels, A. D.; Farkas, Ö.; Foresman, J. B.; Ortiz, J. V.; Cioslowski, J.; Fox, D. J. *Gaussian 09*, revision C.01; Gaussian, Inc.: Wallingford, CT, 2009.
(36) (a) Becke, A. D. *J. Chem. Phys.* **1993**, *98*, 5648−5652. (b) Lee, C.; Yang, W.; Parr, R. G. *Phys. Rev. B* **1988**, *37*, 785−789.
(37) (a) Bühl, M.; Kabrede, H. *J. Chem. Theory Comput.* **2006**, *2*, 1282−1290. (b) Bühl, M.; Reimann, C.; Pantazis, D. A.; Bredow, T.; Neese, F. *J. Chem. Theory Comput.* **2008**, *4*, 1449−1459.
(38) Micera, G.; Garribba, E. *Int. J. Quantum Chem.* **2012**, *112*, 2486−2498.
(39) (a) Miertuš, S.; Scrocco, E.; Tomasi, J. *Chem. Phys.* **1981**, *55*, 117−129. (b) Miertuš, S.; Tomasi, J. *Chem. Phys.* **1982**, *65*, 239−245. (c) Cossi, M.; Barone, V.; Cammi, R.; Tomasi, J. *Chem. Phys. Lett.* **1996**, *255*, 327−335.
(40) (a) Lodyga-Chruscinska, E.; Sanna, D.; Garribba, E.; Micera, G. *Dalton Trans.* **2008**, 4903−4916. (b) Lodyga-Chruscinska, E.; Micera, G.; Garribba, E. *Inorg. Chem.* **2011**, *50*, 883−899.
(41) Sanna, D.; Pecoraro, V.; Micera, G.; Garribba, E. *J. Biol. Inorg. Chem.* **2012**, *17*, 773−790.
(42) (a) Perdew, J. P.; Burke, K.; Ernzerhof, M. *Phys. Rev. Lett.* **1996**, *77*, 3865−3868. (b) Perdew, J. P.; Burke, K.; Ernzerhof, M. *Phys. Rev. Lett.* **1997**, *78*, 1396−1396.
(43) (a) Neese, F. *ORCA - An Ab Initio, DFT and Semiempirical Program Package, Version 2.9*; Max-Planck-Institute for Bioinorganic Chemistry: Mülheim a. d. Ruhr, Germany, 2012. (b) Neese, F. *Wiley Interdiscip. Rev.: Comput. Mol. Sci.* **2012**, *2*, 73−78.
(44) (a) Micera, G.; Garribba, E. *Dalton Trans.* **2009**, 1914−1918. (b) Micera, G.; Pecoraro, V. L.; Garribba, E. *Inorg. Chem.* **2009**, *48*, 5790−5796. (c) Micera, G.; Garribba, E. *Eur. J. Inorg. Chem.* **2010**, 4697−4710. (d) Gorelsky, S.; Micera, G.; Garribba, E. *Chem.—Eur. J.* **2010**, *16*, 8167−8180. (e) Micera, G.; Garribba, E. *J. Comput. Chem.* **2011**, *32*, 2822−2835. (f) Sanna, D.; Buglyó, P.; Bíró, L.; Micera, G.; Garribba, E. *Eur. J. Inorg. Chem.* **2012**, 1079−1092. (g) Micera, G.; Garribba, E. *Eur. J. Inorg. Chem.* **2011**, 3768−3780. (h) Sanna, D.; Varnágy, K.; Timári, S.; Micera, G.; Garribba, E. *Inorg. Chem.* **2011**, *50*, 10328−10341. (i) Pisano, L.; Varnagy, K.; Timári, S.; Hegetschweiler, K.; Micera, G.; Garribba, E. *Inorg. Chem.* **2013**, *52*, 5260−5272. (j) Sanna, D.; Várnagy, K.; Lihi, N.; Micera, G.; Garribba, E. *Inorg. Chem.* **2013**, *52*, 8202−8213. (k) Lodyga-Chruscinska, E.; Szebesczyk, A.; Sanna, D.; Hegetschweiler, K.; Micera, G.; Garribba, E. *Dalton Trans.* **2013**, *42*, 13404−13416.
(45) Hamilton, R. G. *Clin. Chem.* **1987**, *33*, 1707−25.
(46) (a) Gilinskaya, L. *J. Struct. Chem.* **2008**, *49*, 245−254. (b) Gourier, D.; Delpoux, O.; Bonduelle, A.; Binet, L.; Ciofini, I.; Vezin, H. *J. Phys. Chem. B* **2010**, *114*, 3714−3725.
(47) DeKoch, R. J.; West, D. J.; Cannon, J. C.; Chasteen, N. D. *Biochemistry* **1974**, *13*, 4347−4354.
(48) Chasteen, N. D.; DeKoch, R. J.; Rogers, B. L.; Hanna, M. W. *J. Am. Chem. Soc.* **1973**, *95*, 1301−1309.
(49) Smith, T. S.; Root, C. A.; Kampf, J. W.; Rasmussen, P. G.; Pecoraro, V. L. *J. Am. Chem. Soc.* **2000**, *122*, 767−775.
(50) Fitzgerald, J. J.; Chasteen, N. D. *Biochemistry* **1974**, *13*, 4338−4347.
(51) Chasteen, N. D.; Grady, J. K.; Holloway, C. E. *Inorg. Chem.* **1986**, *25*, 2754−2760.
(52) Sun, H. Z.; Li, H. Y.; Sadler, P. J. *Chem. Rev.* **1999**, *99*, 2817−2842.
(53) Buglyó, P.; Kiss, E.; Fábián, I.; Kiss, T.; Sanna, D.; Garribba, E.; Micera, G. *Inorg. Chim. Acta* **2000**, *306*, 174−183.
(54) Rangel, M.; Leite, A.; João Amorim, M.; Garribba, E.; Micera, G.; Lodyga-Chruscinska, E. *Inorg. Chem.* **2006**, *45*, 8086−8097.
(55) Simplaceanu, V.; Lukin, J. A.; Fang, T.-Y.; Zou, M.; Ho, N. T.; Ho, C. *Biophys. J.* **2000**, *79*, 1146−1154.
(56) Kubal, G.; Sadler, P. J.; Tucker, A. *Eur. J. Biochem.* **1994**, *220*, 781−787.
(57) Nishihara, S.; Shimizu, A.; Arata, Y. *Mol. Immunol.* **1986**, *23*, 285−290.
(58) Hu, W.; Luo, Q.; Ma, X.; Wu, K.; Liu, J.; Chen, Y.; Xiong, S.; Wang, J.; Sadler, P. J.; Wang, F. *Chem.—Eur. J.* **2009**, *15*, 6586−6594.
(59) Crans, D. C.; Khan, A. R.; Mahroof-Tahir, M.; Mondal, S.; Miller, S. M.; la Cour, A.; Anderson, O. P.; Jakusch, T.; Kiss, T. *J. Chem. Soc., Dalton Trans.* **2001**, 3337−3345.
(60) Garribba, E.; Micera, G.; Sanna, D. *Inorg. Chim. Acta* **2006**, *359*, 4470−4476.

(61) Hansen, T. V.; Aaseth, J.; Alexander, J. *Arch. Toxicol.* **1982**, *50*, 195−202.
(62) Bruech, M.; Quintanilla, M. E.; Legrum, W.; Koch, J.; Netter, K. J.; Fuhrmann, G. F. *Toxicology* **1984**, *31*, 283−295.
(63) Garner, M.; Reglinski, J.; Smith, W. E.; McMurray, J.; Abdullah, I.; Wilson, R. *J. Biol. Inorg. Chem.* **1997**, *2*, 235−241.
(64) De Cremer, K.; Van Hulle, M.; Chéry, C.; Cornelis, R.; Strijckmans, K.; Dams, R.; Lameire, N.; Vanholder, R. *J. Biol. Inorg. Chem.* **2002**, *7*, 884−890.
(65) Dingley, A. L.; Kustin, K.; Macara, I. G.; McLeod, G. C. *Biochim. Biophys. Acta, Biomembr.* **1981**, *649*, 493−502.
(66) *Williams Hematology*, 8th ed.; The McGraw-Hill Co., Inc.: China, 2010.
(67) Dörnyei, Á.; Marcão, S.; Costa Pessoa, J.; Jakusch, T.; Kiss, T. *Eur. J. Inorg. Chem.* **2006**, 3614−3621.
(68) Zhang, B.; Ruan, L.; Chen, B.; Lu, J.; Wang, K. *BioMetals* **1997**, *10*, 291−298.
(69) (a) Aureliano, M. *Dalton Trans.* **2009**, 9093−9100. (b) Aureliano, M.; Crans, D. C. *J. Inorg. Biochem.* **2009**, *103*, 536−546.
(70) Moore, J. W.; Pearson, R. G. *Kinetic and Mechanism*, 3rd ed.; John Wiley & Sons: New York, 1981.
(71) (a) Simons, T. J. B. *J. Membr. Biol.* **1991**, *123*, 63−71. (b) Simonsen, L. O.; Brown, A. M.; Harbak, H.; Kristensen, B. I.; Bennekou, P. *Blood Cells, Mol., Dis.* **2011**, *46*, 266−276.
(72) Crans, D. C.; Baruah, B.; Ross, A.; Levinger, N. E. *Coord. Chem. Rev.* **2009**, *253*, 2178−2185.
(73) Sabbioni, E.; Kuèera, J.; Pietra, R.; Vesterberg, O. *Sci. Total Environ.* **1996**, *188*, 49−58.
(74) Ishida, O.; Kihira, K.; Tsukamoto, Y.; Marumo, F. *Clin. Chem.* **1989**, *35*, 127−130.
(75) Willsky, G. R.; Halvorsen, K.; Godzala III, M. E.; Chi, L.-H.; Most, M. J.; Kaszynski, P.; Crans, D. C.; Goldfine, A. B.; Kostyniak, P. J. *Metallomics* **2013**, *5*, 1491−1502.
(76) (a) Costa Pessoa, J.; Marques, R. L.; Boas, L. F. V.; Gillard, R. D. *Polyhedron* **1990**, *9*, 81−98. (b) Costa Pessoa, J.; Antunest, J. L.; Boas, L. F. V.; Gillard, R. D. *Polyhedron* **1992**, *11*, 1449−1461. (c) Micera, G.; Sanna, D.; Dessì, A.; Kiss, T.; Buglyó, P. *Gazz. Chim. Ital.* **1993**, *123*, 573−577. (d) Alberico, E.; Dewaele, D.; Kiss, T.; Micera, G. *J. Chem. Soc., Dalton Trans.* **1995**, 425−430. (e) Costa Pessoa, J.; Tomaz, I.; Kiss, T.; Kiss, E.; Buglyó, P. *J. Biol. Inorg. Chem.* **2002**, *7*, 225−240.
(77) Thompson, K. H.; Battell, M.; McNeill, J. H. In *Vanadium in the Environment, Part 2: Health Effects*; Nriagu, J. O., Ed.; Wiley: New York, 1998; pp 21−37.
(78) Rehder, D.; Costa Pessoa, J.; Geraldes, C.; Castro, M.; Kabanos, T.; Kiss, T.; Meier, B.; Micera, G.; Pettersson, L.; Rangel, M.; Salifoglou, A.; Turel, I.; Wang, D. *J. Biol. Inorg. Chem.* **2002**, *7*, 384−396.
(79) Sakurai, H.; Fugono, J.; Yasui, H. *Mini-Rev. Med. Chem.* **2004**, *4*, 41−48.